

EARTH, A GROUND COUPLING PROGRAM AND SIMPLIFIED METHODS
TO PREDICT GROUND HEAT TRANSFER FOR
SEASONAL STORAGE TANKS AND BASEMENTS

by

FRANCIS PAUL CHIARAMONTE III

A thesis submitted in partial fulfillment of
the requirements for the degree of

MASTER OF SCIENCE
(Mechanical Engineering)

at the
UNIVERSITY OF WISCONSIN-MADISON

1982

Acknowledgments

This work could not have been possible without the guidance of Professors Bill Beckman and John Mitchell. I am grateful for their help and constant demand for excellence. I extend my thanks to the staff and fellow graduate students in the Solar Energy Lab for their assistance at the "tough spots," especially Mike Arny and Daryl Erbs.

Outside the technical arena, I wish to express my gratitude to my parents who have always given me substantial encouragement. Also, I give my sincere appreciation to Jenny Ladwig who has been a blessing in her own special way.

The work of this thesis has been funded by the Department of Energy.

creases. On an annual basis, the disagreement is 9% for dry sandy loam soil but this increases to 35% when the soil is one-hundred percent saturated.

	Page
3.1 Introduction	52
3.2 Seasonal Storage Tank	54
3.2.1 Storage Tank Ground Heat Loss: Transient Model Versus Steady State Model	54
3.2.2 Estimation of the Overall Conductance for Steady State Heat Loss (The Shapefactor Model)	65
3.2.3 Storage Tank Ground Heat Loss: Steady State Model Versus Shapefactor Model	76
3.3 Basement	81
3.3.1 Determining a Representative Earth Temperature for the Steady State Models	81
3.3.2 Estimating the Overall Conductance for the Steady State Models	102
3.3.3 Sensitivity Analysis of T_u	111
3.4 Conclusions	113
4.0 SUMMARY, CONCLUSIONS AND RECOMMENDATIONS	121
4.1 The Computer Program EARTH	121
4.2 Simplified Design Models	123
4.3 Recommendations	127
APPENDIX ONE--MATHEMATICAL DERIVATION OF THE SOL-AIR TEMPERATURE	130
APPENDIX TWO--EARTH AS A TRNSYS COMPONENT	132
APPENDIX THREE--GRID CHECK, SELECTED INTERNAL PROGRAM VALUES	151
APPENDIX FOUR--PROGRAM LISTINGS	154
APPENDIX FIVE--TRNSYS DECK	175
BIBLIOGRAPHY	177

LIST OF FIGURES (continued)

<u>Figure</u>		<u>Page</u>
3.2.4	Earth-insulation Conductance Schemes	66
3.2.5	Error of UA_{sf} to UA_{ss} vs. Tank Insulation Thickness	70
3.2.6	Tank Heat Loss Simplification to Describe Parameter Variations Using the Shapefactor Model	73
3.2.7	Maximum Error Between UA_{sf} and UA_{ss}	75
3.2.8	Solar System Performance: Steady State vs. Shapefactor, Case One	78
3.2.9	Solar System Performance: Steady State vs. Shapefactor, Case Two	80
3.3.1	Basement-Soil System to Determine the Overall Conductance, UA_{ss}	84
3.3.2	Undisturbed Earth Temperature, T_u , at Various Depths Compared to the Representative Earth Temperature, T_e , Madison, WI	89
3.3.3	Undisturbed Earth Temperature, T_u at Various Depths Compared to the Representative Earth Temperature, T_e , Charleston, S.C.	91
3.3.4	Basement Energy Requirements, Q_{env} , Madison, WI, $k \text{ soil} = 0.9 \frac{\text{KJ}}{\text{m hr } ^\circ\text{C}}$	93
3.3.5	Basement Energy Requirements, Q_{env} , Madison, WI, $k \text{ soil} = 4.7 \frac{\text{KJ}}{\text{m hr } ^\circ\text{C}}$	94
3.3.6	Basement Energy Requirements, Q_{env} , Madison, WI, $k \text{ soil} = 8.9 \frac{\text{KJ}}{\text{m hr } ^\circ\text{C}}$	96
3.3.7	Basement Energy Requirements, Q_{env} , Charleston, S.C., $k \text{ soil} = 0.9 \frac{\text{KJ}}{\text{m hr } ^\circ\text{C}}$	98
3.3.8	Basement Energy Requirements, Q_{env} , Charleston, S.C., $k \text{ soil} = 4.7 \frac{\text{KJ}}{\text{m hr } ^\circ\text{C}}$	100

LIST OF TABLES

<u>Table</u>		<u>Page</u>
2.3.1	Components for a Solar Space Heating System Using Seasonal Heat Storage	18
2.3.2	Simulated Basement Heat Loss Using a Time-Step of One Hour and Twenty Four Hours, Madison, WI	23
2.4.1	Conductance Array Values for the Earth Structure (Node 73) of Figure 2.4.1	32
2.5.1	Basement Parameters (Program Comparison Case)	49
3.2.1	Assumptions Used For Storage Tank Ground Heat Loss	58
3.2.2	System Parameters (Space Heating)	60
3.3.1	Basement Parameters	82
3.3.2	Annual Basement Heating Requirements, Madison, WI	112
3.3.3a	Parameters Used for T_u , Madison, WI	114
3.3.3b	Variation of Soil Parameters; Effect on Temperature, T_u (°C)	114
3.3.4a	Soil Parameters Used for T_u , Charleston, S.C.	115
3.3.4b	Variation of Soil Parameters; Effect on Temperature, T_u (°C)	115
3.4.1	Summary of the Annual Performance of the Solar Space Heating System Using Seasonal Heat Storage	117
3.4.2	Summary of the Predicted Fraction of the Monthly Heating Load Supplied by Solar Space Heating System	118

h_{amb}	Convective heat transfer coefficient at the ground surface
h_{room}	Convective heat transfer coefficient at the walls of the structure
H_{hor}	Incident, horizontal solar radiation
H_T	Rate of total radiation per unit area incident upon the tilted collector surface
i	First index in an array for node identification
$i+1$	Node to the right of the node concerned
$i-1$	Node to the left of the node concerned
j	Second index in an array for node identification
$j+1$	Node below the node concerned
$j-1$	Node above the node concerned
k	Thermal conductivity
$K_c(\beta)$	Soil thermal conductivity at a given moisture content
k_{earth}	Thermal conductivity of the soil
k_{x_L}	Thermal conductivity between two nodes aligned horizontally and on the left side of the center node
k_{x_r}	Thermal conductivity between two nodes aligned horizontally and on right side of the center node
k_{y_b}	Thermal conductivity between two nodes aligned vertically and on the bottom of the center node
k_{y_t}	Thermal conductivity between two nodes aligned vertically and on the top of the center node
L	Latent heat of vaporization of water
\dot{m}_f	Mass flow rate of fluid
M	Number of heat flow lanes (shape factor)
N	Temperature increments between the isothermal boundaries (shape factor)

\bar{T}	Annual average temperature
T_a'	Environment temperature
$T_a, T_b,$ T_c, T_d	Temperatures between insulation and soil (tank study)
T_{amb}	Ambient temperature
T_{av}	Approximation to the monthly earth temperature (averaging)
T_B	Basement temperature
T_{dp}	Dew point temperature
T_e	Monthly representative earth temperature
T_{es}	Earth structure temperature
T^f	Temperature of node in future time-step
T_g	Ground surface temperature
T_h	Temperature of fluid from heat source
T_i	Inlet temperature
T_L	Temperature of load fluid
T_o	Outlet temperature
T_r	Room temperature
T_s	Fixed sink or ground temperature (tank study)
T_{sa}	Sol-Air temperature
T_{SF}	T_t , predicted by the Shapefactor Model
T_{sky}	Sky temperature
T_{SS}	T_t , predicted by the Steady State Model
T_t	Tank temperature
T_T	T_t , predicted by the Transient Model

1.0 INTRODUCTION

1.1 Background

The potential energy savings of constructing a building totally or partially underground compared to the same structure built above ground have attracted designers and researchers to earth sheltered design and analysis. In the area of energy conservation, there are several advantages to placing a structure below ground. Above-ground structures experience unwanted energy losses or gains to or from the environment by air leakage and conductance [24]. The undesirable energy transfer from air leakage is virtually non-existent in underground structures. The heat transfer from an earth sheltered building by conduction is lower than above-ground structures because the soil adjacent to the earth sheltered building thermally dampens the severe temperature variations of the outside air. Furthermore, this damping is more significant as the depth below grade increases where a constant ground temperature is achieved around ten meters [16]. Additional energy savings can be realized from an underground building because its effective thermal mass encompasses part of the adjacent soil. Buildings with a large thermal capacity, which are partially heated by direct solar heat gain, prevent the interior temperature from changing drastically over short time intervals. Assuming this temperature variation is within or near the comfort zone, heating and cooling requirements are reduced to a minimum.

flexibility, the energy analysis using a computer program was selected.

In this study a computer program was developed which evaluates the ground heat flow from a single story earth sheltered dwelling, a basement completely below grade, a slab of an above grade building, and a fully mixed, sensible energy, in-ground seasonal storage tank. The program meets the following requirements:

1. Both the heat transfer rate from the stated structures to the adjacent soil and the heat transfer rate from the soil to all neighboring boundaries must be modeled and available.
2. The program should be general and inexpensive to use.
3. The required data for the program must be readily available and require minimal computational effort for the user.
4. The physical boundaries for the ground coupled structure must be accurately modeled.
5. The program must be compatible with TRNSYS, a transient simulation program developed at the University of Wisconsin which predicts the thermal performance of systems under transient conditions.

Several existing programs meet some of these conditions, but not all of them. For example, a program developed at the University of Toronto by Hooper [9] et al. models the thermal performance of solar space heating systems using annual heat storage. However, this pro-

1.2 Purpose

This thesis is divided into two general sections. The first section, Chapter 2, describes the assumptions used and explains the programming logic of the transient, ground heat transfer program EARTH. The major thermal processes of the soil adjacent to the below ground structure, which influence the structure's energy performance, are simplified and expressed numerically for computer use. Since EARTH is used in conjunction with TRNSYS, compatibility of the two programs is presented. In order to gain a clear understanding, a complete sequential presentation of EARTH is described.

The second section, Chapter 3, presents simplified techniques to estimate the monthly ground heat transfer from basements and sensible energy, fully mixed, seasonal storage tanks. Simulation of thermal performance for a solar space heating system using a seasonal storage tank is studied at a northern location in the United States. System performance is compared by calculating the tank heat loss in two forms. First, the tank heat loss is approximated by a lumped steady state model [22], then the tank heat loss is computed based on a transient finite difference model of the soil surrounding the tank. The steady state technique assumes the ground heat loss flows between the varying tank temperature and a fixed sink temperature through a combined earth-insulation conductance. A method to estimate the combined earth-insulation conductance is presented. The thermal performance of a basement is studied at a northern and southe-

2.0 EARTH, A GROUND COUPLING PROGRAM

2.1 Introduction

In this chapter the Program EARTH, which determines the heat flow for in-ground structures, is described. First, selection of significant soil characteristics are justified. Then a brief explanation of the necessary TRNSYS subprograms to be used with EARTH for transient system evaluation is presented. A major portion of the chapter is devoted to a sequential description of EARTH. Finally, simulation results as computed by EARTH are compared to the results determined by a ground coupling program developed at another university.

In Section 2.2 the primary mechanisms which influence the thermal behavior of the soil surrounding an underground structure are analyzed. The analysis begins with the soil being non-isotropic and non-homogeneous with transient, three dimensional, heat and mass transfer. The significance of each thermal mechanism is evaluated. As a result, the transient, heat transfer assumptions used in EARTH are justified.

Section 2.3 discusses the required TRNSYS subprograms, components, to be used with EARTH for performance evaluation of thermal systems displaying transient behavior. The TRNSYS components for a solar space heating system using an underground seasonal storage tank are presented. Also, the components required to predict ground

3. an on grade slab of an above ground structure having a fixed interior temperature where the ground heat loss calculations are evaluated through the slab.
4. A one story earth sheltered dwelling having any desired fixed interior temperature such that the ground encloses all sides except one (for entrance from the outside). Ground heat loss calculations are evaluated on the ceiling, back wall (opposite the wall exposed to the ambient conditions) and floor.

The program EARTH can be naturally divided into three parts. The first part calculates values which are constant for the entire simulation, the second part calculates values that are constant during a time-step, and the third part calculates values which are constant during a time-step but may be needed several times during a time-step for other TRNSYS [1] components. Each part is explained in detail.

In Section 2.5 the validity of EARTH is discussed. Thermal performance results of a completely below grade basement calculated by EARTH are compared to the results computed by a ground coupled heat transfer program developed at Georgia Institute of Technology.

The objective of this chapter is to justify the heat transfer modes used in EARTH and discuss the role of EARTH with respect to TRNSYS. Also, to present the program logic in a clear and concise manner and to illustrate the validity of EARTH.

$$k(\beta) = k_c(\beta)$$

2.2.2

This equation is used for all subsequent ground heat flow analyses.

2.2.2 Latent Heat of Fusion

The latent heat of fusion, namely the energy release during freezing and thawing, has been studied by Hooper using a one dimensional numerical model for soil below a snow covered layer. Although latent heat of fusion in the soil with a snow cover reduces the frost penetration depth and slightly dampens winter soil temperature extremes [6], the following result was concluded. "Although the inclusion of latent heat of fusion in the model changes the temperature of the soil, it makes less than one percent difference to the yearly net heat transfer into the ground when the initial and final soil temperatures are the same" [6]. Therefore, latent heat of fusion will not be included in this ground heat flow study.

2.2.3 Groundwater Transport Mechanisms

MOISTURE MIGRATION: The influence of moisture migration on soil thermal conductivity was studied by Moench and Evans [5] for sandy loam soils at several soil moisture contents. Taking measurements at 24°C, the component of thermal conductivity due to moisture movement never exceeded five percent. Since the neighboring soil temperature of the earth structures considered does not go significantly higher than 24°C, it can be concluded that the impact of moisture migration on changing the soil conductivity value is small.

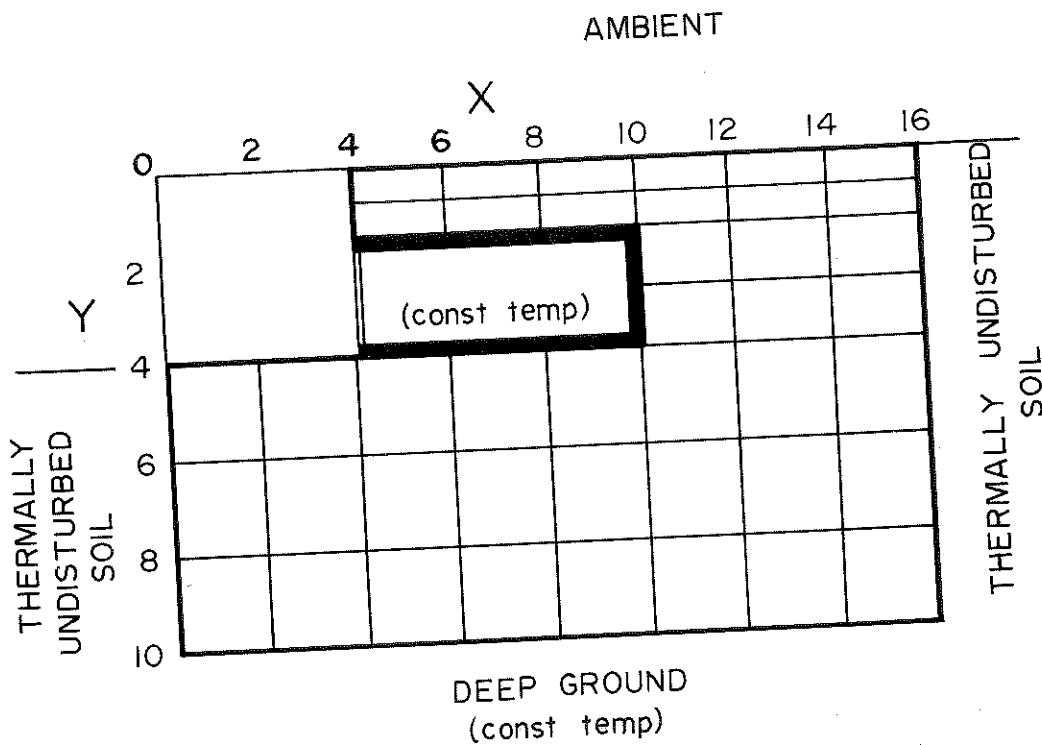
Appendix Two.

2.2.4 Classification

Based on the preceding analysis of the soil surrounding the earth structure, determining the ground heat flow has been simplified. The heat flow can be evaluated mathematically by assuming the earth structure-soil system represents a propagation boundary value problem [11], since the dependent variable, temperature, is a function of time and space variables. However, modeling the distributed parameter, dynamic system in this manner involves three dimensional, partial differential equations. Due to computational expense and the preceding simplifications, the earth structure-soil system is governed by the following two dimensional, conduction heat transfer equation [15]:

$$\rho c_p \frac{\partial T}{\partial t} = \frac{\partial}{\partial x} \left(\frac{k \partial T}{\partial x} \right) + \frac{\partial}{\partial y} \left(\frac{k \partial T}{\partial y} \right) \quad 2.2.3$$

This equation represents the balance between the energy storage rate of the soil on the left side of the equation to the net rate of energy from conduction on the right side. To solve numerically, the partial differential equations are reduced to an equivalent set of equations in finite difference form. The space variables, x and y , are subdivided, forming an earth grid. The temperature distribution through the soil is calculated by assuming a constant temperature at each grid point for a specified, brief time interval. Each grid



Position	Non-Symmetric Case		Mechanism
Horizontal	$T(x,0,t) = f(t)$	x between 4 and 10	Weather data
	$T(x,4,t) = f(t)$	x between 0 and 4	" "
	$T(x,10,t) = T_{dg}$		Deep ground temp
Vertical	$T(0,y,t) = g(t)$	y between 4 and 10	Undisturbed soil
	$T(4,y,t) = f(t)$	y between 0 and 1.5	Weather data
	$T(16,y,t) = h(t)$		Undisturbed soil
Earth Structure	$T(x,1.5,t) = T_{es}$	x between 4 and 10	Earth Structure temp
	$T(10,y,t) = T_{es}$	y between 1.5 and 4	" " "
	$T(x,4,t) = T_{es}$	x between 4 and 10	" " "

T = Temperature, t = time, x,y in meters

Figure 2.2.1 Earth Grid as an Initial Value Problem - Earth Sheltered Dwelling

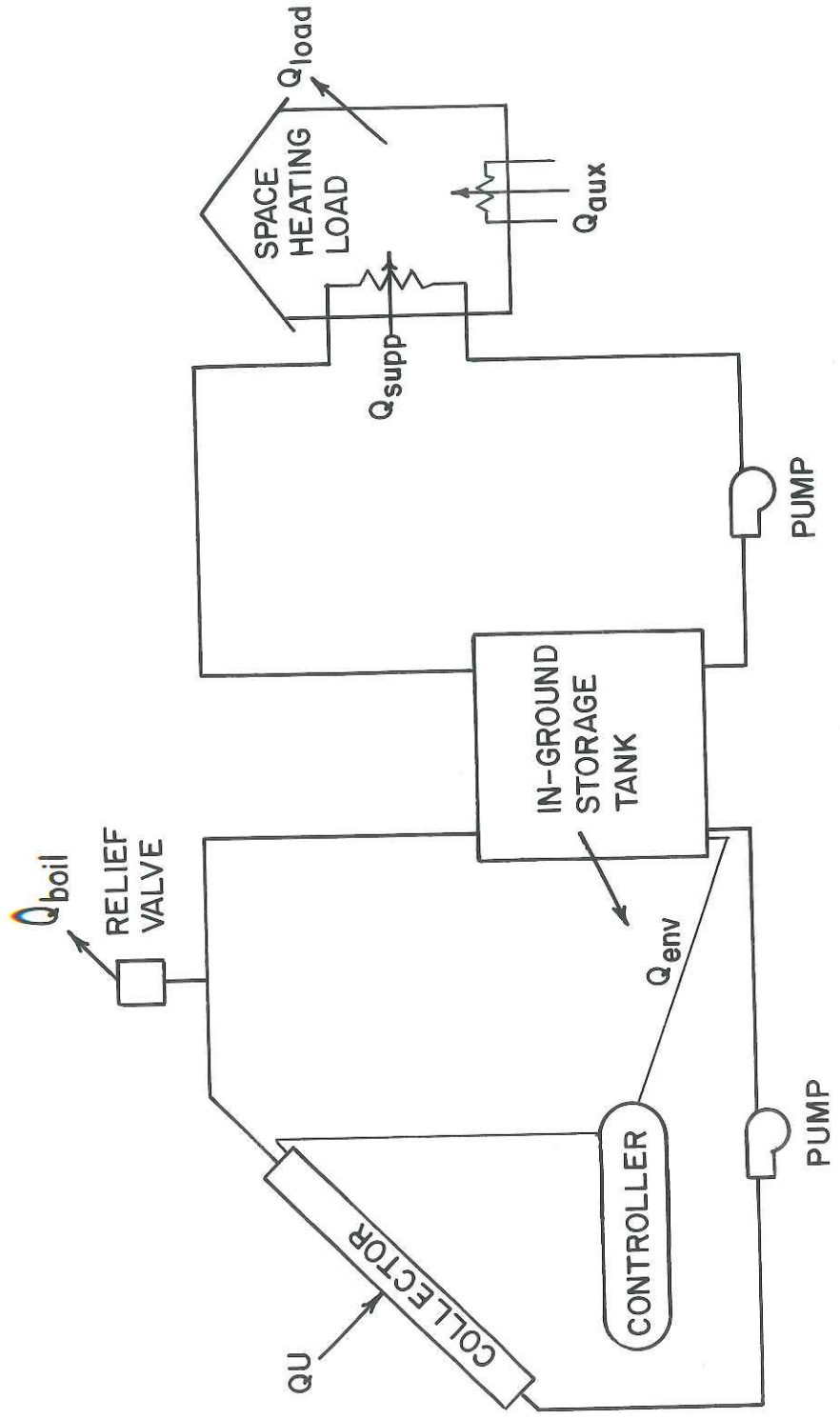


Figure 2.3.1 Schematic of a Ground Coupled Solar Space Heating System [14]

ing inputs, and the number of derivatives or time dependent differential equations involved. The components of the system are linked by interconnecting selected output of one component to input of another component. For example, the fluid flow rate leaving a pump (output) in a collector-storage tank loop becomes the input fluid flow rate to the solar collector.

DATA READER: Simulations use formatted hour by hour Solmet TMY weather data [19]. Specifically, data for global solar radiation on a horizontal surface, dry bulb temperature and dew point temperature were utilized.

RADIATION PROCESSOR: One of this component's capabilities is to estimate the radiation incident on a tilted surface given horizontal radiation values. The Erbs correlation [18] was selected to estimate the isolation on the collector surface, where ground reflectance, ρ , latitude of the system, ϕ , collector slope, β , and azimuth angle, γ , were fixed during a simulation.

FLAT PLATE SOLAR COLLECTOR: The net rate of useful energy from a collector is expressed by the Hottel and Whiller equation [7]:

$$\dot{Q}U = A_c F_r [H_T(\tau\alpha) - U_L(T_i - T_{amb})] = (\dot{m}C_p)_f (T_o - T_i) \quad 2.3.1$$

which states that the total rate of energy collected ($\dot{Q}U$) is the rate of energy absorbed by the collector minus the rate of energy lost to the environment. The collector is assumed to have constant optical properties, $\tau\alpha$, overall loss coefficient, U_L , and collector efficiency factor, F' , during a simulation.

is above a specified maximum, T_{\max} , and will not operate if the temperature difference is below a specified minimum value, T_{\min} . When the collector-tank temperature difference is within the dead bank, T_{\max} to T_{\min} , the pump is turned on if the fluid leaving the collector is heating up and is turned off if the fluid is cooling down.

PUMP: Necessary to maintain a mass flow rate, the pump in the collector-storage tank loop establishes the fluid flow rate. In this case the pump uses a specified maximum flow rate while on.

ENERGY/SPACE HEATING LOAD: Among other capabilities, this component estimates the residential space heating load expressed by the equation [1]:

$$\dot{Q}_{\text{LOAD}} = UA_h(T_t - T_{\text{amb}}) \quad 2.3.3$$

neglecting internal energy gains. The room temperature, T_r , is set to 20°C, the varying air temperature is represented by T_{amb} , and UA_h is the heating requirement of the residence, which remains constant during the simulation.

2.3.2 Time Step Features

The Solmet weather data [19] used in the simulation for the thermal systems described is available in one hour intervals. With this weather data, a maximum time-step of one hour can be used. However, accurate results, using a larger time step, can be obtained for heat transfer predictions of a basement, slab or earth sheltered dwelling. Because of this, a computational and cost saving proce-

TABLE 2.3.2 Simulated Basement Heat Loss Using a Time-step
of One Hour and Twenty Four Hours, Madison, Wisconsin.
Thermal Conductivity of Soil = $8.9 \frac{\text{KJ}}{\text{hr m } ^\circ\text{C}}$
Basement Wall Insulation Thickness = 0.0254 m

<u>Month</u>	<u>$\Delta t = 1 \text{ hr}$ Q(GJ)</u>	<u>$\Delta t = 24 \text{ hr}$ Q(GJ)</u>	<u>% Error</u>
Jan	3.200	3.138	1.94
Feb	3.097	3.045	1.68
Mar	3.309	3.264	1.36
Apr	2.701	2.667	1.26
May	2.231	2.205	1.17
Jun	1.616	1.596	1.24
Jul	1.246	1.231	1.20
Aug	1.128	1.122	0.53
Sep	1.187	1.188	0.08
Oct	1.600	1.607	0.44
Nov	1.951	1.960	0.46
Dec	2.666	2.678	0.45

structure wall (if applicable) and at the ground surface. Also, initial temperature for the earth structure, left boundary condition nodes (if earth sheltered dwelling) and right boundary condition nodes is required; an added option is to enter node numbers to obtain node temperature history print-out. In order to determine the dimensions of the earth structure and neighboring soil, a hand drawn diagram is necessary. Except for the earth sheltered dwelling shown in Figure 2.4.1, only half of the earth structure-soil system must be drawn. A typical configuration will have 70 parameters; however, no additional data sets are necessary. The intention is to input values that require minimal computational effort for the user.

NODE NUMBERING INTEGER VARIABLE VALUES: Node numbering and computation of thermal soil properties has eliminated the need for the user to calculate the conduction and capacitance matrices. Important nodes are numbered internally, such as corner nodes, and nodes near the boundaries. These node numbers are stored and used to identify a specific location (x, y) on the earth grid. Node location is essential to accurately assign the conductance between nodes.

CALCULATIONS: The earth grid is divided into three major zones, and each zone may have a different soil thermal conductivity and capacity shown in Figures A.2.6 and 7 of Appendix Two. For a specific zone all nodes are the same size. The program computes four thermal capacities, one for each of the three soil zones and

one for the tank (if used) expressed by the equation:

$$CAP = \rho C_p V \quad 2.4.1$$

CAP represents the thermal capacity, ρ the density, C_p the specific heat, and V the node volume. Except for the tank, the earth structure temperature is fixed at any desired value, whereby the capacitance of the structure is not considered. Realistically, this fixed temperature may be thought of as energy rate control. Energy rate control assumes there is exactly enough energy added or removed from the earth structure to maintain the fixed temperature. Since only ground coupled heat transfer is considered for the basement, slab or earth sheltered dwelling, the rate of energy required to maintain a fixed temperature is equal to the rate at which energy is leaving the earth structure (\dot{Q}_{env}) to the adjacent soil.

Nineteen combinations of thermal conductances in EARTH symbolized as COND1. . .COND19 model all possible conductances encountered by the large number of nodes in an earth grid. These values consider conduction and convection at the following locations: the ground surface, interior soil, insulation, earth structure material, and earth structure fluid, as shown in Figures 2.4.2 and 2.4.3. Using finite difference, the one dimensional lumped thermal conductance, COND, is:

$$COND = \frac{kA}{x} \quad 2.4.2$$

Thermal conductivity is k , the node area on one face is A , and x is

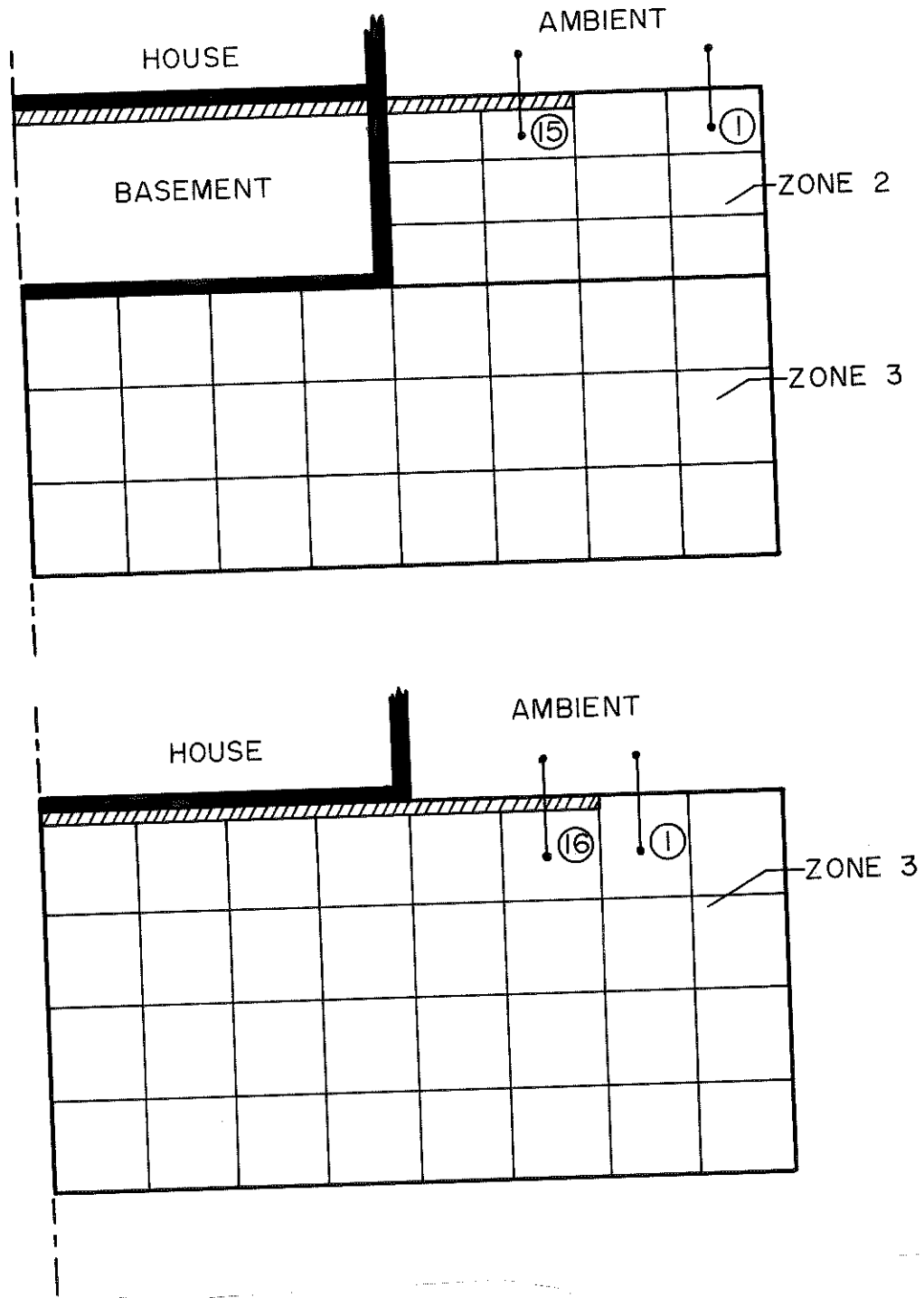
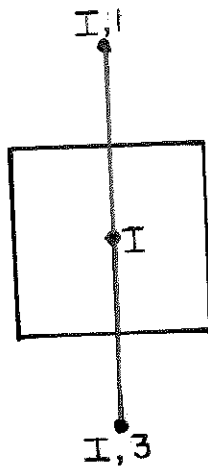
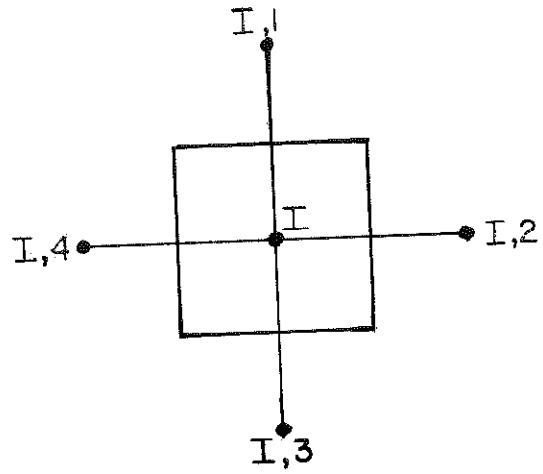


Figure 2.4.3 Additional Conduction Values for Basement and Slab



Boundary condition nodes: 1 dimensional case



Earth nodes: 2 dimensional case

Earth structure: 2 dimensional case

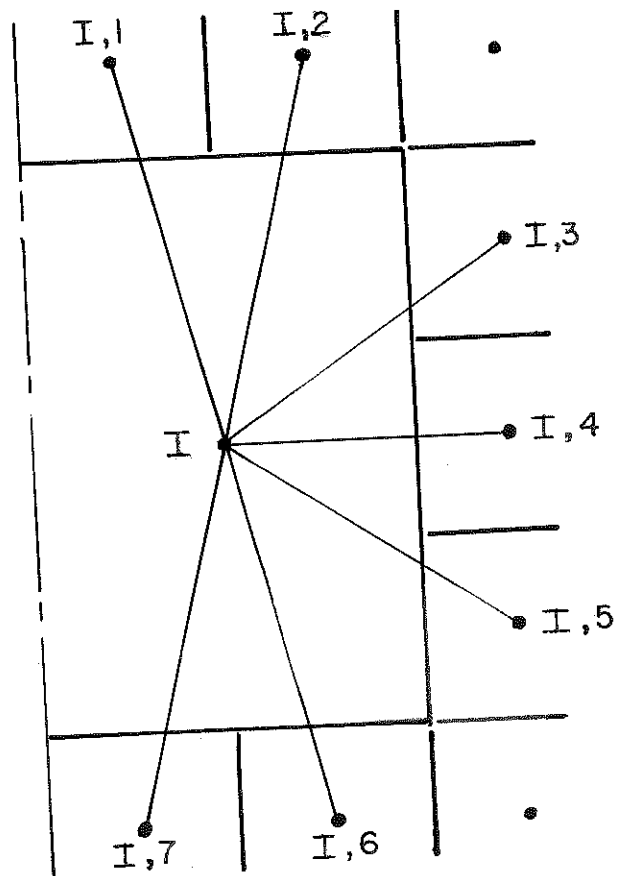


Figure 2.4.4 Conduction Arrangement Between Nodes

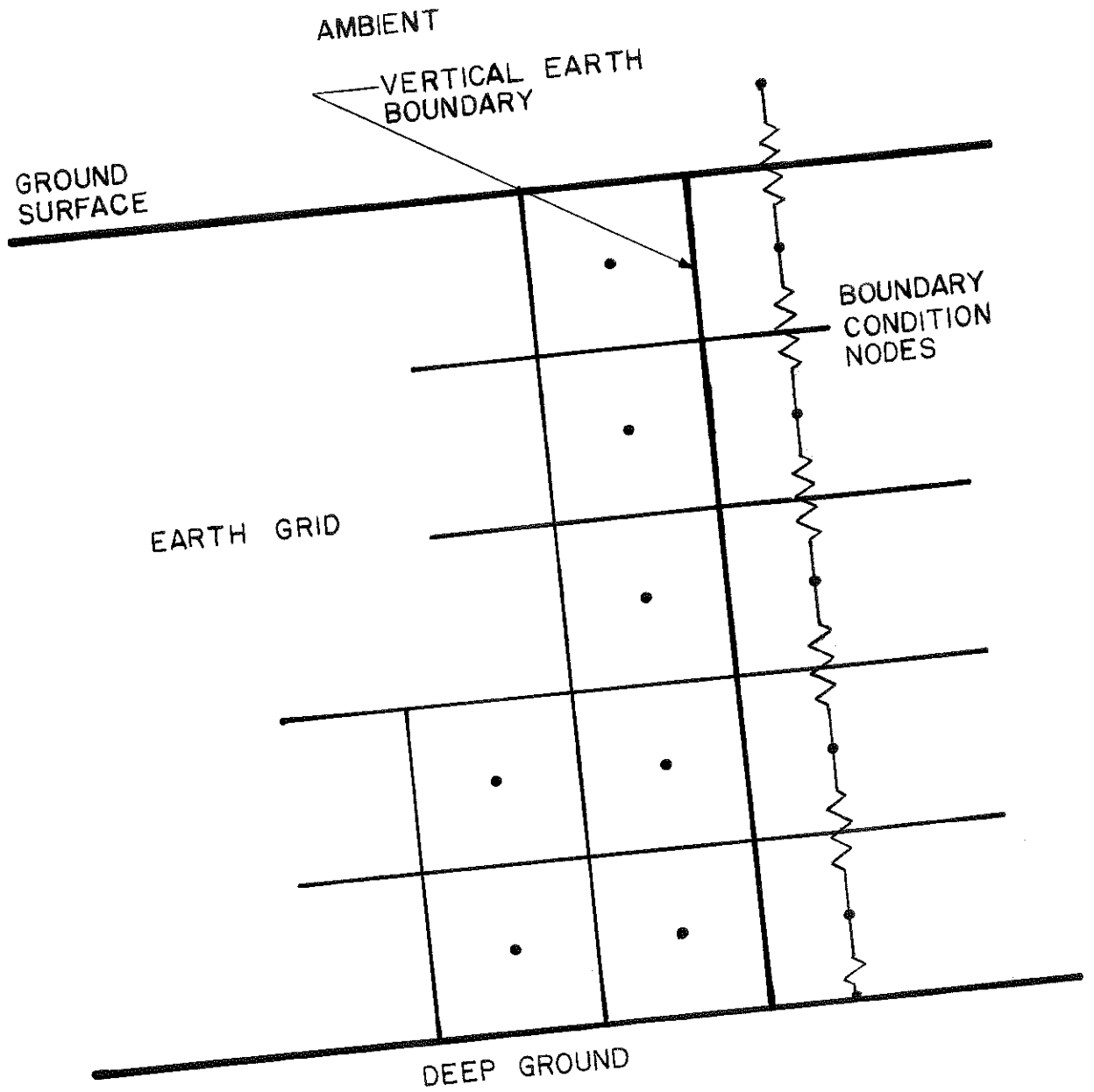


Figure 2.4.5 Conduction Arrangement to Model Vertical Earth Boundaries

boundary, left boundary (earth sheltered dwelling), deep ground and ambient. These nodes correspond to nodes 73 through 88 in Figure 2.4.1. The remaining grid points are initialized by equating the initial temperature of a right boundary condition node to all nodes in the corresponding row. This continues down the right boundary condition column of nodes until the entire earth grid is initialized. Specifically, in Figure 2.4.1 nodes 1 through 8 are initialized by the temperature of node 74, nodes 9 through 16 by 75, and so on to nodes 62 through 72 being initialized by the temperature of node 82.

GRID CHECK: If the results of a simulation are questionable, selected internal program values can be printed by placing a negative sign in front of the first parameter. This checking procedure will allow errors, from grid numbering and conduction calculation, to be detected easier and faster. These internal program values are defined in Appendix Three.

2.4.2 First Call in Time-Step

The second part of the program is called only once during a time-step, since an explicit numerical integration method is employed. This part includes system inputs and nodal temperature assignment.

INPUTS: The inputs to the program consist of temperatures for the ambient, deep ground and dew point, and solar radiation on a horizontal surface for all structures. The buried storage tank requires temperatures and mass flow rates from the heat source and load. The slab, basement, or earth sheltered dwelling requires a fixed temperature implying energy rate control; also, the basement uses a

explicit formulation was selected. For a given node, I, the neighboring node temperature values are assigned in the second index, J. Specifically, the two dimensional, temperature array (I, J) for node 28 in Figure 2.4.1 is assigned as follows: (I,1) is the temperature of node 24, (I,2) is the temperature of boundary condition node 78, (I,3) is the temperature of node 39 and (I,4) is the temperature of node 27. There are always four nodes surrounding a grid point, except for the earth structure, shown in Figure 2.4.4, which generally has more neighboring earth nodes. The earth structure is modeled as a single node at a fixed temperature for the slab, basement on earth sheltered dwelling; a varying temperature for the storage tank.

As previously discussed, the soil temperature at the vertical boundaries of the earth grid model undisturbed earth. Knowledge of earth temperatures at various depths becomes unnecessary other than an initial guess in the parameter list. If the earth grid is made large enough, the undisturbed earth approximation becomes accurate for this two dimensional, temperature distribution analysis. The earth grid is the proper size if less than ten percent of its total heat flow is through these vertical boundaries [17].

SOL-AIR TEMPERATURE: Similar to other earth nodes, the ground surface nodes must have four neighboring nodes for temperature assignment. To account for radiation exchange, at the earth's surface, the sol-air temperature, T_{sa} , as shown in Figure 2.4.6, is used. The sol-air temperature is described as [1]:

That temperature of the outdoor air which, in the absence of all radiation exchanges, would give the same rate of heat entry into the surface as would exist with the actual combination of incident solar radiation, radiant energy exchange with the sky and outdoor surroundings and convective heat exchange with the outdoor air.

A mathematical definition of the sol-air temperature, T_{sa} , is derived in Appendix One. In the program, this value is stored in the $T(I,1)$ location and is used for temperature evaluation between the ambient and ground surface nodes.

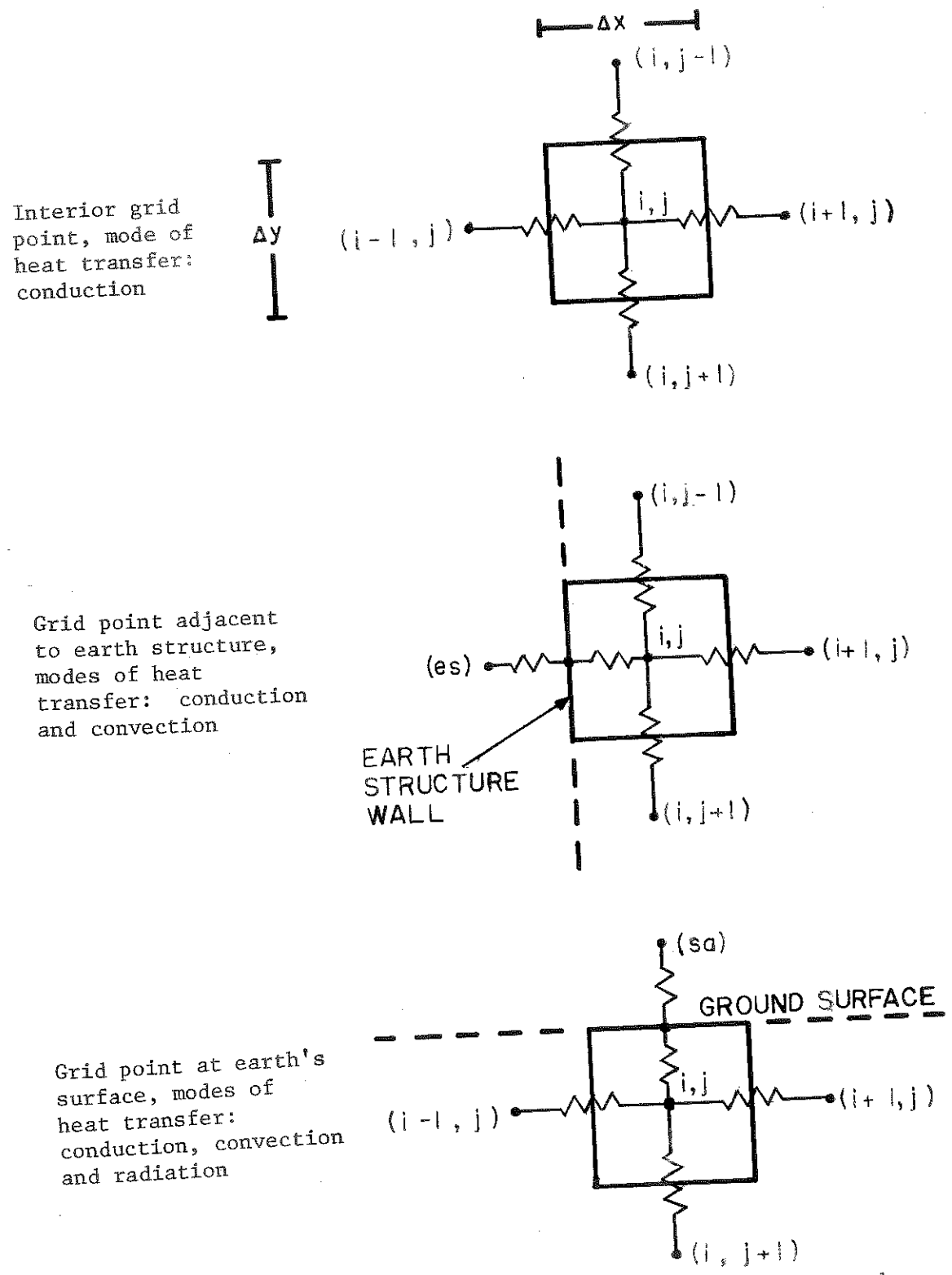
2.4.3 Iterative Call in Time-Step

This part of the program is called several times during a time-step, since other TRNSYS [1] components described in Section 2.3.1 use an iterative numerical method to estimate the dependent variable. This part includes the algorithm and heat transfer calculations.

NON-STEADY STATE NUMERICAL METHOD: In order to compute the heat flow for the earth structure, the energy exchange between the earth nodes must be determined. The differential heat transfer expression (Equation 2.2.3) is solved numerically by employing the forward difference approximation. This numerical technique is described in terms of temperature for one nodal point, at a given x and y location. Predicting the temperature profile through time for a single node becomes [11]:

$$T^f = T + \int_t^{t^f} f(T,t)dt \quad 2.4.7$$

where T^f and t^f are the new temperature and time values respectively. T and t are the present temperature and time values respectively and



Interior grid point, mode of heat transfer: conduction

Grid point adjacent to earth structure, modes of heat transfer: conduction and convection

Grid point at earth's surface, modes of heat transfer: conduction, convection and radiation

Figure 2.4.7 Finite Difference Representation of Selected Nodes in Earth Grid

$$T_{ij}^f = T_{ij} + \frac{\Delta t}{(\rho C_p)_{ij}} \left\{ \left[\frac{k_{x_r} (T_{i+1,j} - T_{i,j})}{x_{i+1} - x_i} + \frac{k_{x_l} (T_{i-1,j} - T_{i,j})}{x_{i-1} - x_i} \right] \Delta Y + \left[\frac{k_{y_b} (T_{i,j+1} - T_{i,j})}{y_{j+1} - y_j} + \frac{k_{y_t} (T_{i,j-1} - T_{i,j})}{y_{j-1} - y_j} \right] \Delta X \right\} \quad 2.4.10$$

For an earth node adjacent to the earth structure, convection and conduction are modeled. The temperature for this node is updated in the following manner [27]:

$$T_{ij}^f = T_{ij} + \frac{\Delta t}{(\rho C_p)_{ij}} \left\{ \left[\frac{k_{x_r} (T_{i+1,j} - T_{i,j})}{x_{i+1} - x_i} + \left(\frac{1}{\frac{1}{h_{room}} + \frac{1}{2} \frac{(x_{i-1} - x_i)}{k_{x_l}}} \right) (T_{es} - T_{i,j}) \right] \Delta Y + \left[\frac{k_{x_b} (T_{i,j+1} - T_{i,j})}{y_{j+1} - y_j} + \frac{k_{y_t} (T_{i,j-1} - T_{i,j})}{y_{j-1} - y_j} \right] \Delta X \right\} \quad 2.4.11$$

At the ground surface the modes of heat transfer are conduction, convection and radiation. The new temperature for a node at the surface is computed by the following expression [27]:

2.4.16

$$\dot{Q}_U = (\dot{m}_h C_p) (T_h - T_t)$$

and the energy rate to the load is:

2.4.17

$$\dot{Q}_{\text{supp}} = (\dot{m}_L C_p) (T_L - T_t)$$

Thus, the future tank temperature can be obtained by solving the energy balance of Equation 2.4.13 for T^f .

HEAT TRANSFER: For the basement, tank or earth sheltered dwelling, the heat flow rate from the top, \dot{Q}_t , side, \dot{Q}_s , and bottom, \dot{Q}_b , of the structure can be calculated; a negative sign represents heat flow out of the structure. For the slab, the heat which flows from the interior air through the slab to the ground is computed. The rate of heat transfer between the earth grid and boundary conditions can be determined and is divided into the following categories, where a negative sign represents heat leaving the earth grid: right boundary, \dot{Q}_{rbc} , left boundary, \dot{Q}_{lbc} , (earth sheltered dwelling) deep ground, \dot{Q}_{gsink} , and ambient, \dot{Q}_{asink} , as shown in Figure 2.4.9.

OUTPUT: The output consists of the earth structure temperature, flow rates to the heat source and load for the tank, heat flow through the top, side and bottom of the earth structure, right boundary, left boundary, deep ground and ambient (earth's surface) of the earth grid. Additionally, the earth grid critical time-step and user selected nodal temperatures may be printed as output. All output values are defined in Appendix Two.

2.5 Comparing the Results of EARTH

To test the accuracy of the program, the energy demand of a basement located in Madison, Wisconsin is computed using EARTH. These results are compared to the computations using a ground heat transfer program developed at Georgia Institute of Technology (G.I.T.) [30]. The basement temperature is fixed at 20°C and insulation is placed over the full length of the basement walls at a thickness of 0.076 meters (three inches), as shown in Figure 2.5.1. Basement and soil specifications, boundary conditions and other pertinent parameters are listed in Table 2.5.1.

The program developed in G.I.T. assumes quasi-steady state, two dimensional ground heat flow. Monthly averaged values are calculated on a steady state basis. The temperature profile through the soil and basement heat transfer is evaluated using a finite element formulation [28]. The temperature distribution at the vertical earth boundary of Figure 2.5.1 is computed using Flucker's equation [28]:

$$T(y,t) = T_{\infty} + 15e^{-0.1896y} \sin(0.1726t + 0.1896y - 1.54) \quad 2.5.1$$

when T represents temperature, y the soil depth and t the day of the year starting from December 31.

The monthly energy requirements of the basement as predicted by EARTH and the G.I.T. program are shown in Figure 2.5.2. On an annual basis the computed basement heating demand using EARTH is twenty two percent greater than that calculated using the G.I.T. program. Furthermore,

TABLE 2.5.1 Basement Parameters (Program Comparison Case)

Basement dimensions (m)	0.15
Floor thickness	0.30
Wall thickness	2.1
Height	4.3
Width	
Temperature ($^{\circ}\text{C}$)	20.0
T_{room}	10.0
$T_{\text{deep ground}}$	
Convective heat transfer coefficient ($\frac{\text{KJ}}{\text{m}^2 \text{ hr } ^{\circ}\text{C}}$)	20.5
h_{room}	94.0
h_{amb}	
Thermal conductivity ($\frac{\text{KJ}}{\text{m hr } ^{\circ}\text{C}}$)	4.8
k_{concrete}	0.13
k_{ins}	4.18
k_{soil}	
Thermal capacity ($\frac{\text{KJ}}{\text{m}^3 ^{\circ}\text{C}}$)	1400.0
$(\rho C_p)_{\text{soil}}$	

EARTH does not predict a cooling load in July as indicated by the predictions using the G.I.T. program.

Each program uses a different approach to calculate ground heat flow; therefore, the disagreement in the basement heat transfer can be expected. There are two major differences between the programs. EARTH considers the capacitance of the soil, whereas the G.I.T. program does not. Also EARTH computes the undisturbed earth temperature profile using a one dimensional, semi-infinite slab model, but the G.I.T. program uses equation 2.5.1 to compute the temperature distribution of this boundary. The influence of soil capacitance on basement heat transfer is apparent in Figure 2.5.2. As indicated by the predictions using EARTH, the presence of capacitance results in the amplitude of the heat flow curve being dampened and a two month phase shift to the right as compared to the quasi-steady state G.I.T. curve.

soil at varying moisture contents. The tank insulation thickness, underground tank depth and water table are among the parameters varied in the analysis.

Section 3.3 investigates several steady state heat flow methods to predict the heat transfer between a completely below grade basement and the surrounding soil. The steady state methods are compared to the computer simulated heat flow calculated by the program EARTH. Comparisons are analyzed for a basement in Madison, Wisconsin, and Charleston, South Carolina, for three separate soil conditions. The basement is simulated with insulation of several thicknesses, including zero, covering the walls.

The governing energy balance used in the steady state methods assumes the basement heat flow is simplified in the following manner. The basement heat transfer is thermally driven by the temperature potential between a fixed basement temperature, T_b , and a monthly varying earth temperature, T_e . The heat flows through a lumped conductance, UA_{SS} , which encompasses the basement insulation and some fraction of the surrounding soil. Two methods are developed to approximate the monthly varying earth temperature and are referred to as T_{av} and T_u . Replacing T_e , by each of these earth temperature approximations, in the governing steady state energy balance defines the first two steady state methods. In addition to approximating T_e , a technique to estimate the overall conductance is presented. Using this estimated conductance with each of the earth temperature approximations, two additional steady state methods are developed. Finally,

is assumed to be a right circular cylinder with the height equal to its diameter and the tank is well insulated [14]. Evaluation of the storage tank heat loss rate using Equation 3.2.1 will be referred to as the steady state model.

Using EARTH, the constant overall conductance for ground heat loss, UA_{ss} , can be determined for the in-ground seasonal storage tank. The UA_{ss} value is calculated by constructing an earth grid from the adjacent soil assuming there is one fixed temperature at the ground surface, the vertical boundary and the deep ground with another fixed temperature for the storage tank. The tank-soil system with the desired amount of insulation is shown in Figure 3.2.1 for half of the tank and adjacent soil. When this configuration reaches equilibrium, indicated when the tank heat loss rate does not change with time, the UA_{ss} value can be readily calculated from Equation 3.2.1. Using the described tank-soil system to find UA_{ss} , the assumption that the earth's surface and the deep ground are fixed at the same temperature is based on the concept that on an annual average these two temperatures are approximately equal [16]. Since the actual heat flow from the storage tank goes only to the earth's surface and the deep ground, the vertical boundary is placed far away from the storage tank with a maximum of ten percent of the total heat flow leaving the storage tank crossing its boundaries, thereby causing minimal error in the computation of the overall conductance, UA_{ss} .

When using EARTH to predict the storage tank ground heat loss rate, the tank geometry is rectangular, but it is assumed that the

results are similar to a right circular cylinder of the same length and surface area. It has been observed by Hooper that "fin effects" [9] exist such that the heat loss rate at the corners of the storage tank increases relative to the tank walls. Nevertheless, it is assumed that this will not significantly affect the following results. Also, since EARTH determines two dimensional heat flow for a rectangular tank, the ground heat loss rate on the front and back tank walls is neglected. When evaluating tank heat loss using Equation 3.2.1, a surface area, corresponding to four walls of the rectangular storage tank used in EARTH, is computed for an unbiased comparison. Differences between the transient assumptions concerning the storage tank used in EARTH and the steady state assumptions for the storage tank in Braun's design method are listed in Table 3.2.1.

As described in Chapter 2, the program EARTH calculates tank heat loss using a transient finite difference technique for the heat transfer by conduction in the soil surrounding the tank. Evaluation of the tank heat loss rate using the program EARTH will be referred to as the transient model.

The solar space heating system using seasonal heat storage, as shown in Figure 2.3.1, is used in this analysis. Simulated performance of the system, for a year in Madison, Wisconsin, is compared using two different methods to predict tank heat loss. Thermal performance of the system for the first method is simulated using TRNSYS for the entire heating system with "steady state" tank losses as described in Section 2.2.5. In the second method the performance of the

space heating system is also simulated using TRNSYS, but the performance of the tank is calculated by the program EARTH rather than the subprogram called TYPE4 in TRNSYS.

Comparing simulated performance of the space heating system with the steady state model to the performance with the transient model is calculated for two cases. Each case is distinguished by the tank parameters. The tank of the solar space heating system is tested under the same load, weather conditions and water table depth, but varying significantly in the tank geometry and soil conditions. The unique physical parameters of case one, purposefully selected to minimize the differences, are as follows:

1. Dry soil surrounding the storage tank
2. Well insulated storage tank
3. Storage tank buried deep in the soil
4. Small storage tank surface area (compared to case two)

For case two, the physical parameters were selected to maximize the differences between the steady state model and the transient model and are as follows:

1. Wet soil surrounding the storage tank
2. Marginally insulated storage tank
3. Storage tank buried below grade, but near the ground surface
4. Large storage tank surface area (compared to case one)

A complete list of the solar space heating system parameters is found in Table 3.2.2.

Solar space heating system performance using the steady state model with the favorable parameters of case one yielded good agreement with the transient model. As shown in Figure 3.2.2a, the storage tank temperature predictions are virtually the same throughout the year. The annual fraction of energy supplied by the solar space heating system to the load differs by less than one percent; however, monthly values vary as much as three percent, as illustrated in Figure 3.2.2b. Comparison of the storage tank ground heat loss in Figure 3.2.2c reveals a one percent annual difference, but monthly values have a maximum deviation of forty-six percent in March. This deviation is not too significant since the storage tank ground heat loss represents only five percent of the total energy leaving tank during March; the remainder is supplied to the load.

The less favorable physical parameters of case two produce noticeable differences between the steady state model and the transient model. Although Figure 3.2.3a shows reasonable accuracy for tank temperature prediction, the estimated fraction of the space heating load supplied by the solar system shown in Figure 3.2.3b reveals an annual difference of three percent and a maximum monthly difference of sixteen percent in February. Storage tank ground losses vary by less than three percent annually, but the maximum monthly deviation is thirty-three percent in February as shown in Figure 3.2.3c. This monthly difference is more significant than in case one since the storage tank ground heat loss is thirty-eight percent of the total energy leaving the storage tank.

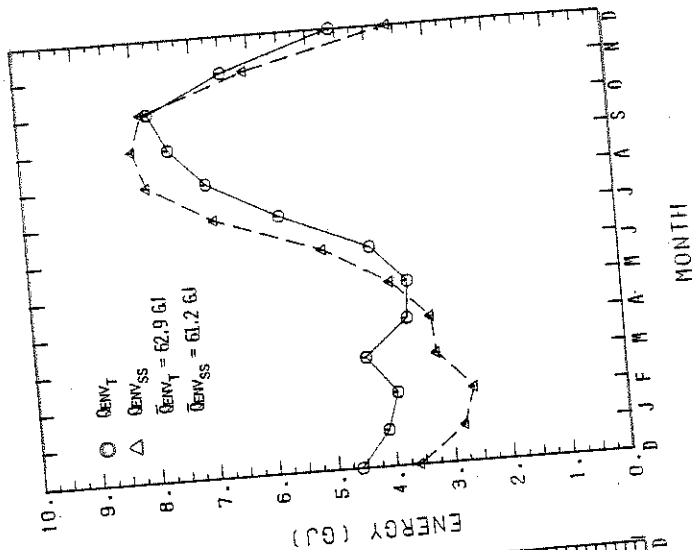


Figure 3.2.3a Tank temperature history

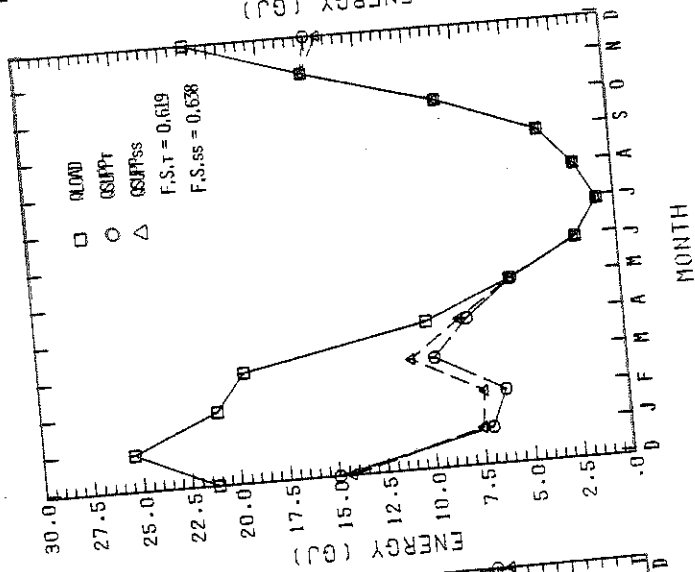


Figure 3.2.3b Solar energy supplied to load

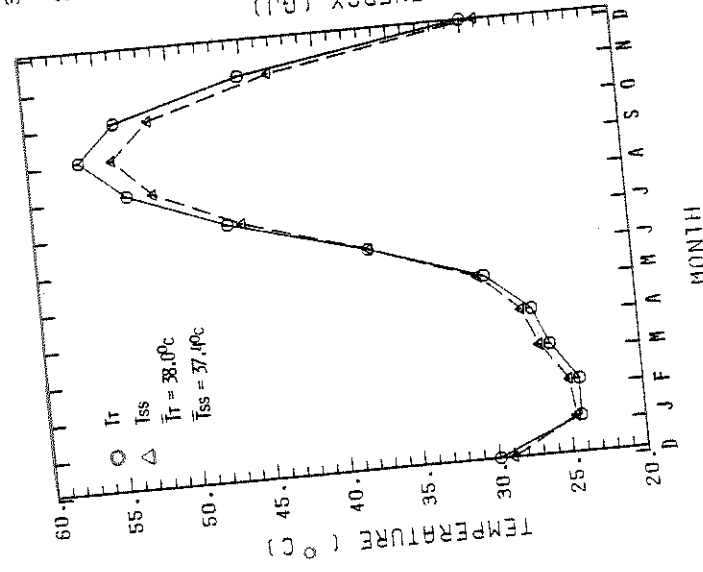


Figure 3.2.3c Tank heat loss history

Figure 3.2.3 Solar System Performance: Transient vs. Steady State, Case Two

conductance, UA_{SS} , via computer. The following section will present a method to calculate UA_{SS} by hand. However, evaluation of UA_{SS} is difficult since soil conditions are time and location dependent.

3.2.2 Estimation of the Overall Conductance for Steady State Heat Loss (The Shapefactor Model)

In order to assign a value to the overall conductance UA_{SS} , used in the steady state model, the individual contributions of the insulation and the earth to this conductance will be evaluated. Consider the lumped conductance separated into two conductances, as shown in Figure 3.2.4, assuming each conductance can be expressed in one dimensional form. One conductance represents the tank insulation for which properties are known, the other conductance represents the earth which is a function of local thermal soil properties and time of year. The problem of estimating the combined earth-insulation conductance is reduced to evaluating the earth conductance.

To approximate the earth conductance consider the earth adjacent to the tank, excluding the insulation, to be enclosed by two isotherms. The storage tank perimeter between the insulation and soil is fixed at a temperature, T_w , and the earth's surface, vertical earth boundary and deep ground are fixed at another temperature, T_s , as shown in Figure 3.2.1 except that the tank isotherm is on the outside of the insulation. If accurate lines of constant temperature and heat flow can be drawn between the two isotherms, T_w and T_s , the conduction shape factor, S , can be evaluated. The number of heat flow lanes, M , and the number of temperature increments between

the isothermal boundaries, N , defines the shape factor by the relationship [21]:

$$S = M/N \quad 3.2.2$$

From this graphical derivation approximating the earth's conductance, UA_{earth} can be determined based on the shape factor and the thermal conductivity of the earth, k_{earth} , being expressed as:

$$UA_{\text{earth}} = k_{\text{earth}}(S) \quad 3.2.3$$

The advantage of using the shape factor to express the conductance of the earth is simply that the shape factor is not a function of the soil properties, but merely the shape of the tank-soil system. If the geometric parameters are known, such as the water table depth, tank shape, and depth buried in the soil, the shape factor can be computed.

As an alternative to graphical methods, the earth conductance can be calculated by using the program EARTH. This is done by constructing an earth grid with the isothermal boundaries T_w and T_s enclosing soil only and allowing this tank-soil system to reach equilibrium. The steady state energy flow rate, \dot{Q}_{earth} , of this system is expressed as:

$$\dot{Q}_{\text{earth}} = UA_{\text{earth}}(T_w - T_s) \quad 3.2.4$$

and the earth conductance, UA_{earth} , can be readily calculated.

mum value, but the agreement will improve as the UA_{ins} value continues to increase.

The shapefactor model is compared to the steady state model for a given storage tank size varying tank insulation thickness, soil properties, water table depth, and tank depth below grade. Consider a $250m^3$ rectangular seasonal storage tank having the dimensions $5m \times 5m \times 10m$ buried 1.25 meters below the earth's surface with a water table of ten meters. Since the geometric properties are fixed, only one simulation using EARTH is required to determine the shapefactor, S . Therefore, the shapefactor conductance of Equation 3.2.5, necessary for the shapefactor model, is easily calculated for any insulation thickness or soil conductivity. However, for the steady state model, the combined earth-insulation conductance must be computed by EARTH for every variation investigated.

The difference between the lumped conductance computed for the shapefactor model to that computed for the steady state model is shown in Figure 3.2.5a as a function of tank insulation thickness for three soil conditions. Although at different tank insulation thicknesses, all three soil conditions considered have a maximum error of five percent for computing the overall conductance, UA_{ss} , using the shapefactor conductance, UA_{sf} . Also, it has been observed that this maximum error occurs when the contribution of the tank insulation, as defined in Equation 3.2.6, to the total shapefactor conductance, of Equation 3.2.5, is fifty percent. Thus, the approx-

imation of an isothermal outer tank wall used in the shapefactor model is least accurate for this condition. The wet soil having a large conductance needs only a thin layer of tank insulation to reach the maximum error, whereas the dry soil having a much smaller conductance requires 0.2 meters of insulation to reach the maximum error. Since it is generally recommended to use 0.2 to 0.3 meters of insulation on the seasonal storage tank [6, 9], and since most soils surrounding a tank can be approximated by the twenty-five percent saturated sandy loam soil, estimating the overall conductance, UA_{ss} , using the shapefactor conductance, UA_{sf} , yields an error of about three percent.

The difference between the overall conductance and the shapefactor conductance is also calculated for a tank with slightly different physical parameters. The tank has the same size and depth below the ground surface, but the water table depth is increased from ten meters to nineteen meters, lessening the thermal influence on the tank from the deep ground horizontal boundary as shown in Figure 3.2.5b. The earth grid constructed from the soil surrounding the tank is larger than the earth grid used for the ten meter water table condition, thereby decreasing the earth conductance used in the shapefactor conductance and requiring more tank insulation to reach the maximum deviation between the overall conductance, UA_{ss} , and the shapefactor conductance UA_{sf} . Comparing Figure 3.2.5a to Figure 3.2.5b, the maximum error values are shifted slightly to the right because of this increased earth grid size. More noticeably, the

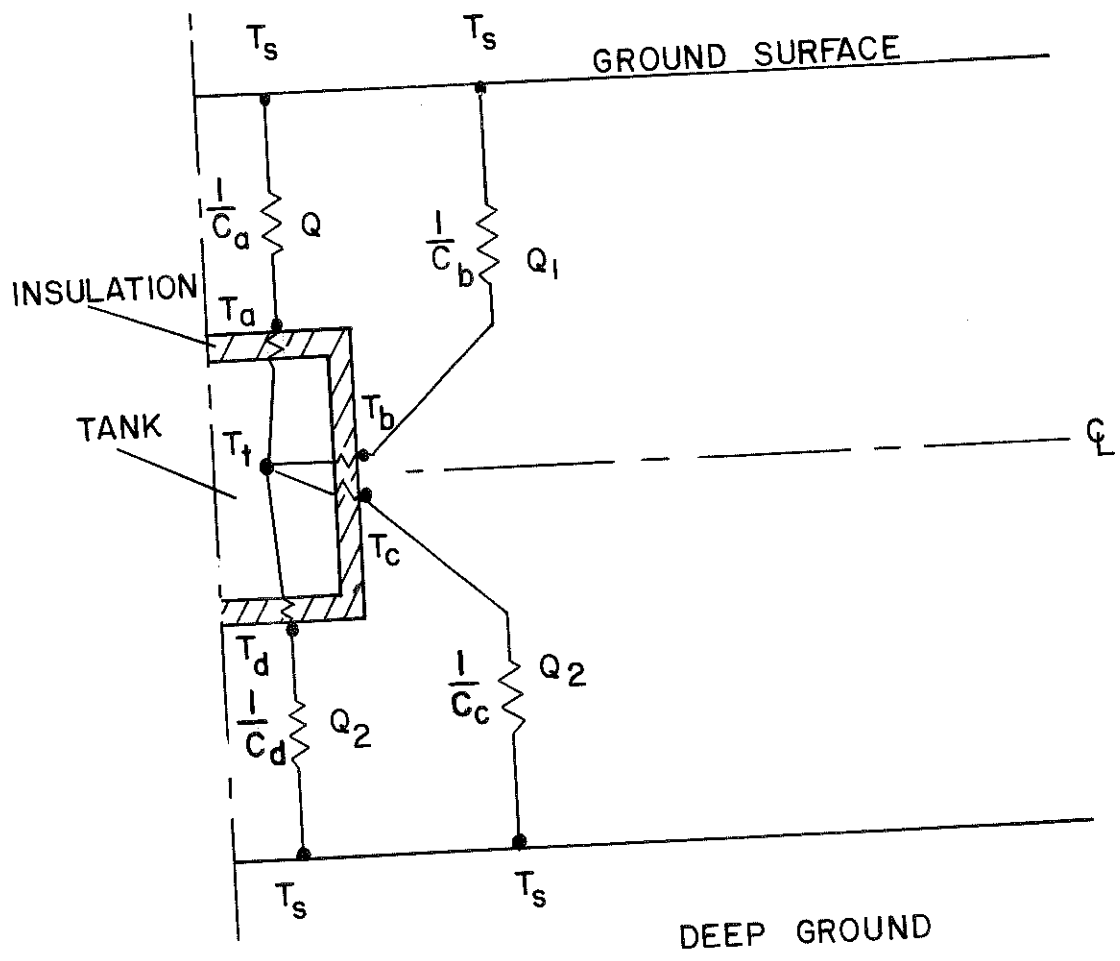


Figure 3.2.6 Tank Heat Loss Simplification to Describe Parameter Variations using the Shapefactor Model

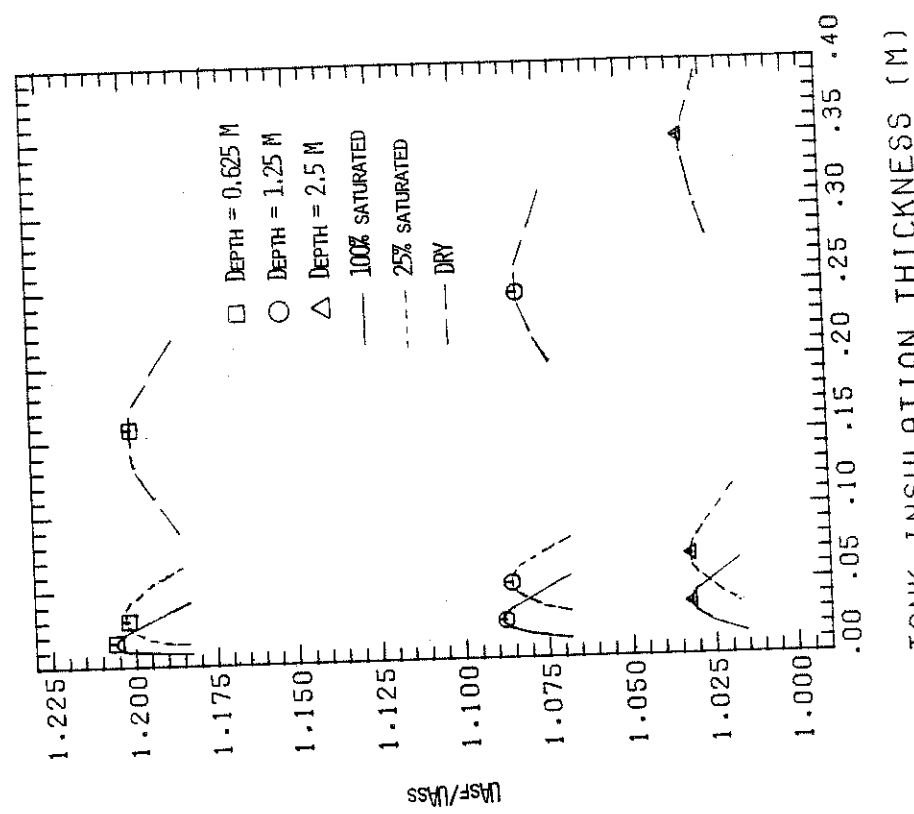


Figure 3.2.7a Error vs. ground depth to tank centerline, 19m water table

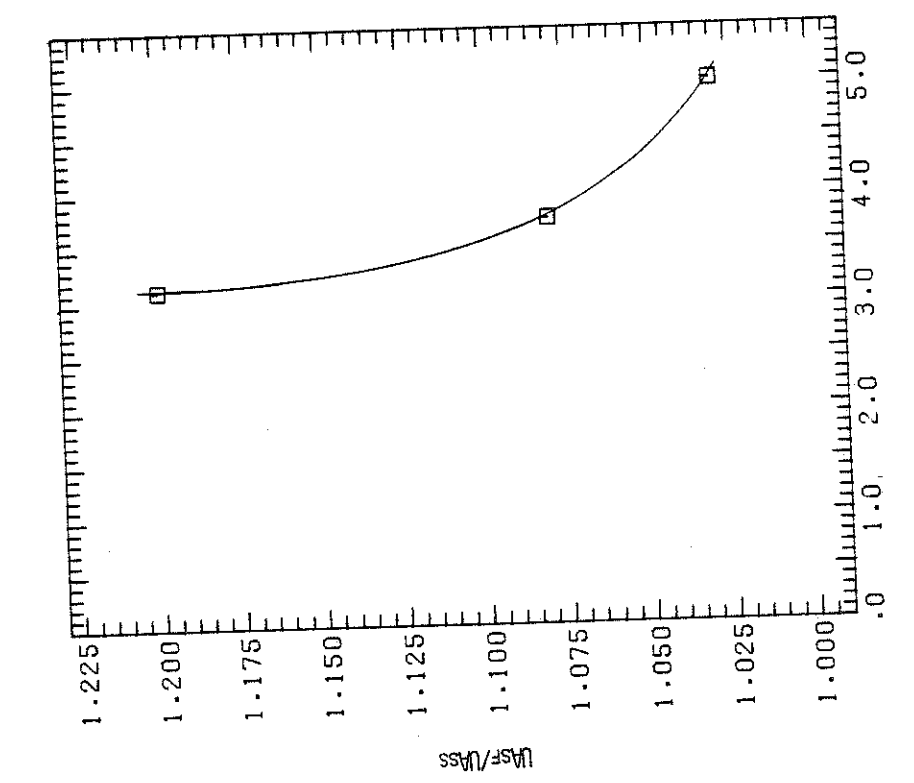


Figure 3.2.7b Error vs. insulation thickness, 19m water table

Figure 3.2.7 Maximum Error Between UASf and UAss

Madison, Wisconsin, and the two models are compared twice. First, the two models are evaluated when the tank is simulated under the condition of case one, and second, the two models are evaluated when the tank is simulated under the conditions of case two; both cases are discussed in Section 3.2.1.

For the favorable parameters of case one, the constant overall conductance of the shapefactor model, UA_{sf} , is only 1.02 times the overall conductance used in the steady state model, UA_{ss} , expressed as:

$$UA_{sf} = 1.02(UA_{ss})$$

3.2.8

Comparing the steady state model to the shapefactor model to predict system performance, case one reveals the storage tank temperature, shown in Figure 3.2.8a, being virtually the same on an annual average, but varying by three degrees celcius on a monthly basis. The fraction of the heating load supplied by the solar space heating system differs by two percent annually; however, the monthly values have a maximum difference of eight percent in February as indicated in Figure 3.2.8b. A direct comparison of the shapefactor model to the steady state model can be made from storage tank ground heat loss predictions, illustrated in Figure 3.2.8c. Annually, the difference is less than one percent, but monthly there is a five percent maximum difference.

For the storage tank in case two having undesirable physical parameters, the constant overall conductance for the shapefactor

model is 1.2 times the overall conductance used for the steady state model, expressed as:

$$UA_{sf} = (1.20)UA_{ss} \quad 3.2.9$$

This increased disagreement between the lumped conductance values is primarily due to the storage tank being nearer to the ground surface, illustrated in Figure 3.2.7a, compared to case one. Comparing the steady state model to the shapefactor model when used to predict system performance in case two, the storage tank temperature of Figure 3.2.9a differs by two degrees celcius annually and a maximum of four degrees celcius monthly. The fraction of the load met by solar energy shows a seven percent annual difference and a twenty percent maximum monthly difference, illustrated in Figure 3.2.9b. As shown in Figure 3.2.9c, the storage tank ground heat loss is consistently overpredicted by the shapefactor model compared to the steady state model. Annually, the tank heat loss difference is twelve percent with a maximum monthly deviation of seventeen percent which occurs in March when twenty-eight percent of the energy leaving the storage tank flows to the surrounding soil. For annual comparison, replacing the steady state model by the shapefactor model yields reasonable space heating performance predictions. However, the true test of the shapefactor model is to compare it with the transient model; this is discussed in the conclusion, Section 3.4. Also, direct numerical comparison of the solar space heating system performance using the transient, steady state and shapefactor

models to estimate the storage tank ground heat loss is listed in Tables 3.4.1 and 3.4.2.

3.3 Basement

3.3.1 Determining a Representative Earth Temperature for the Steady State Models

As described in Section 2.4, basement heat flow to and from the adjacent ground can be readily determined from the program EARTH. In this section, basement heat flow simulated by EARTH will be referred to as the transient model. Basement heat transfer using the transient model will be compared to several simplified methods which assume monthly steady state conditions. Since EARTH is a two dimensional program, the heat flow between the ground, and front and back walls of the basement is not considered. All steady state models used for comparison do not consider this portion of the basement-ground heat flow.

For all comparisons the basement temperature is held constant at 20°C; additional basement parameters are found in Table 3.3.1. Since the thermal properties of soils for a specific location can vary with time, this basement analysis considers several soil conditions at a given location. Sandy loam soil was selected and is used when dry, twenty-five percent saturated and one hundred percent saturated. Although sandy loam soil may not be adjacent to the basement, the wide range of thermal properties for the three soil conditions en-

compass most of the thermal properties of other soil types. As indicated from this study, the type of soil surrounding the basement will have a significant influence on the basement energy demand.

The predicted heat transfer, Q_{env} , between the basement and the adjacent soil for the steady state models is defined by the quasi-steady state energy balance in the following form:

$$Q_{env} = UA_{ss} (T_B - T_e) 24N_o \quad 3.3.1$$

The basement-soil energy exchange is assumed to flow between the basement temperature, T_B , and a monthly representative earth temperature, T_e , through an overall conductance, UA_{ss} . The UA_{ss} value is a lumped conductance consisting of the basement insulation and some portion of the neighboring soil. Time is represented by $24N_o$, where 24 is the hours in a day and N_o is the number of days in a month. Since the overall conductance, UA_{ss} , for the basement-soil system is unknown, this value must be evaluated. UA_{ss} can be calculated by the program EARTH using the system shown in Figure 3.3.1. The soil and insulation for this configuration are enclosed by two isotherms and an adiabatic boundary, similar to the tank-soil system of Section 3.2. Using EARTH, this system is allowed to reach equilibrium, indicated when the basement heat flow does not change with time. The overall conductance can be computed with Equation 3.3.1, using the steady state heat flow and the temperature difference as defined by the two isotherms.

With the overall conductance value calculated and the basement temperature given, proper estimation of the monthly representative earth temperature, T_e , must be evaluated for Equation 3.3.1 to be a valid model. Two methods are presented to approximate T_e .

AVERAGING: The first method to approximate the earth temperature does not depend upon the thermal properties of the soil surrounding the basement. The earth temperature is expressed as the average of the monthly average air temperature, T_{mo} , and the annual average air temperature, T_{ann} , for a specific location. This definition for the earth temperature will be called T_{av} as defined in the following relationship [23]:

$$T_{av} = (T_{mo} + T_{ann})/2 \quad 3.3.2$$

Approximating T_e by T_{av} is of interest since the necessary information is readily available from weather data [19]. Evaluating the earth temperature by Equation 3.3.2 to be used for basement heat transfer calculations was obtained from the residential heating load program, F-LOAD version 3.1 [23]. Basement heat flow calculated by Equation 3.3.1, but replacing T_e by T_{av} will be referred to as the steady state averaging (SSA) model.

UNDISTURBED EARTH: The second method to approximate T_e includes several characteristics of the earth surrounding the basement. Furthermore, this method was not originally intended to yield an earth temperature for basement heat flow calculations. Instead this temperature represents the monthly average temperature, T_u , for a

$$P = PO + \sqrt{\frac{\pi}{Dt}} x$$

3.3.5

Thus, T_u at any depth is defined in terms of four parameters, three of which are location dependent, A_a , BO , and PO , and one that is soil dependent, D .

Varying all parameters for each basement-soil system and geographic location requires a large number of values for each of the parameters. It is desirable to reduce the number of parameters, but still provide a reasonable estimation of T_e . The value of T_u for each location will always be influenced by the annual average earth temperature, A_a . However, since this temperature may not be readily available, the definition of A_a will be changed. In this study A_a is equal to the annual average air temperature which can be easily determined from weather data [19]. This new definition of A_a is nearly equal to the old definition, the average annual earth temperature [16]. To eliminate D as a parameter, a thermal diffusivity of $0.0023 \frac{m^2}{Hr}$ ($0.025 \frac{ft^2}{Hr}$), as recommended by Kusuda and Achenbach [16], will be used regardless of soil type.

In order to reduce the number of independent variables even further, a single soil depth will be assumed. The desired depth must yield a temperature profile, T_u , comparable to the actual temperature profile, T_e . The soil depth was selected by testing several depths for two United States locations. T_u is computed at depths of 1.2, 1.8 and 2.4 meters in Madison, Wisconsin, and Charleston, South Carolina, using the A_a , PO , and BO values, nearest

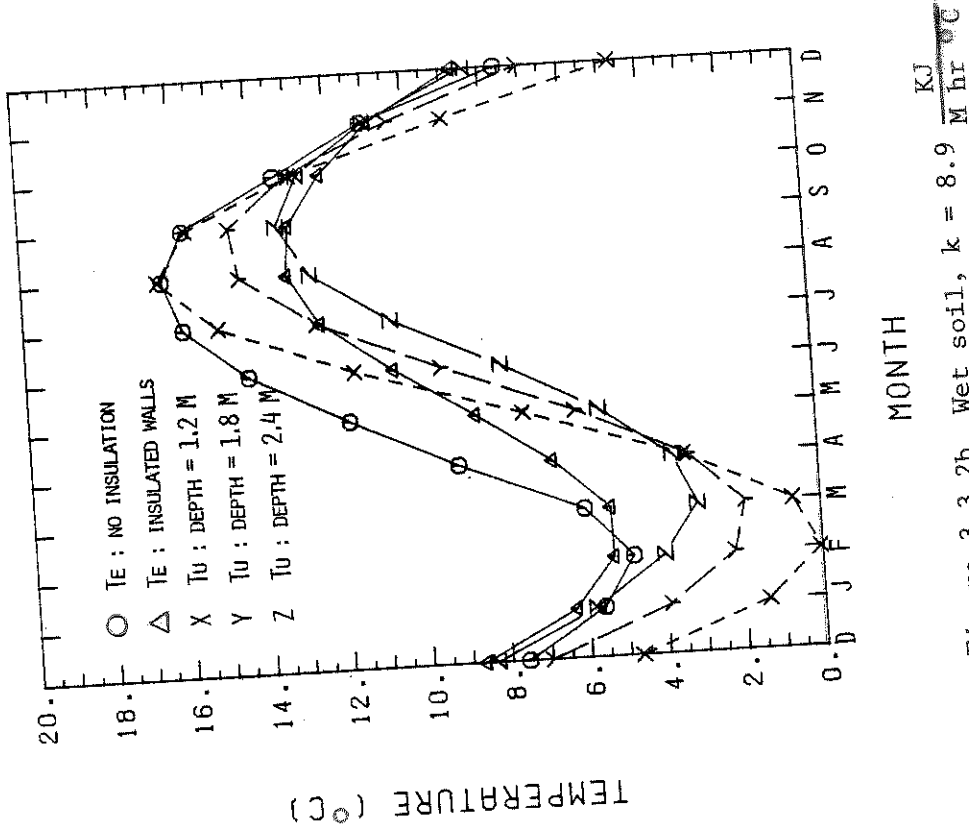


Figure 3.3.2a Dry soil, $k = 0.9 \frac{\text{KJ}}{\text{M hr } ^\circ\text{C}}$

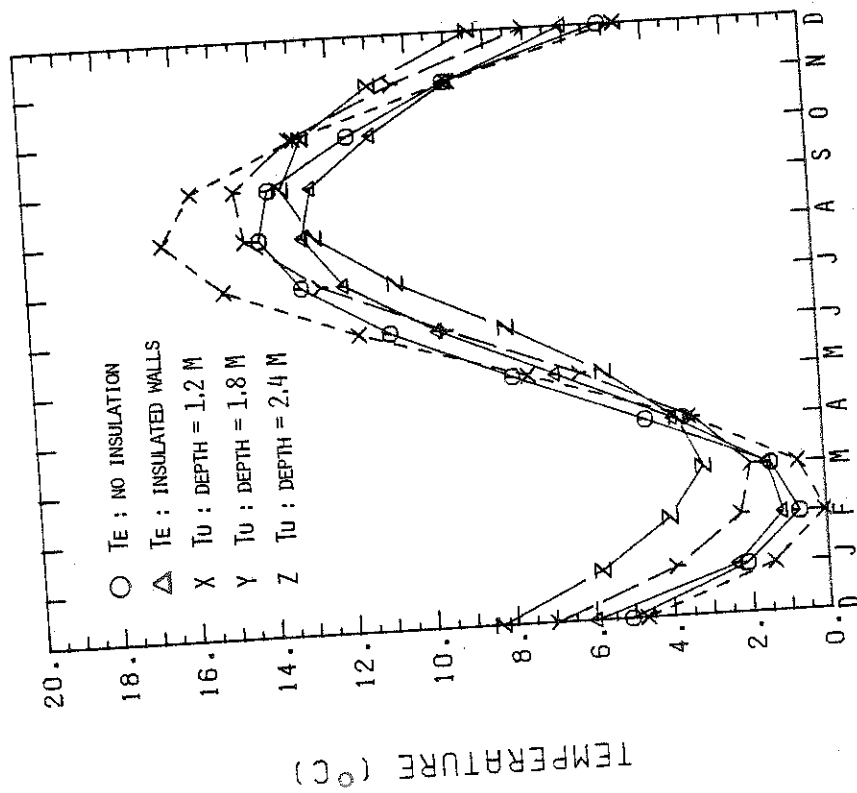


Figure 3.3.2b Wet soil, $k = 8.9 \frac{\text{KJ}}{\text{M hr } ^\circ\text{C}}$

Figure 3.3.2 Undisturbed Earth Temperature, Tu, at Various Depths Compared to the Representative Earth Temperature, Te, Madison, WI

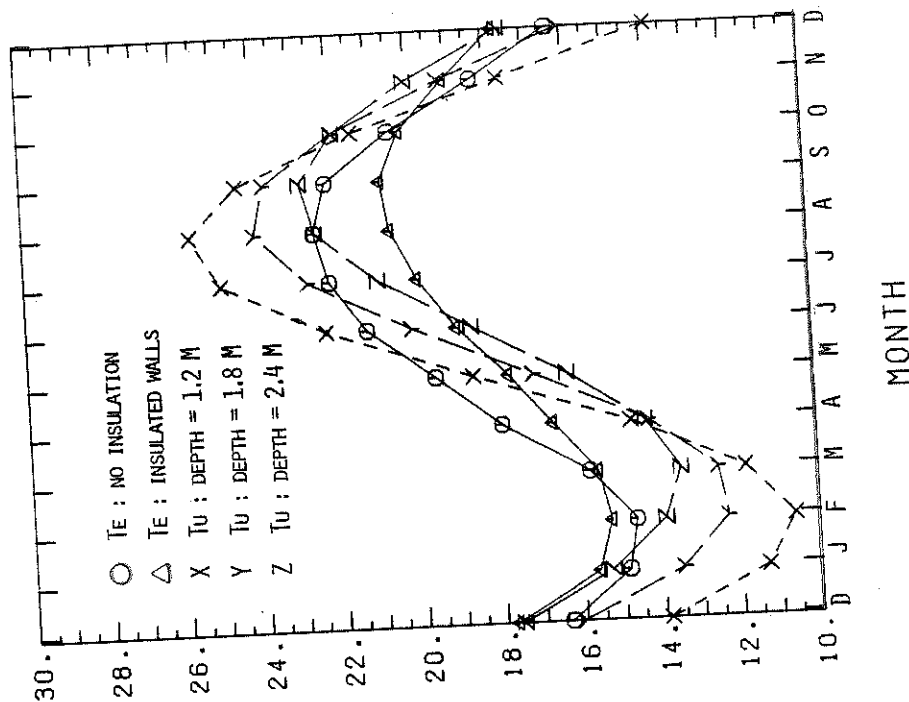


Figure 3.3.3a Dry soil, $k = 0.9 \frac{\text{KJ}}{\text{M hr } ^\circ\text{C}}$

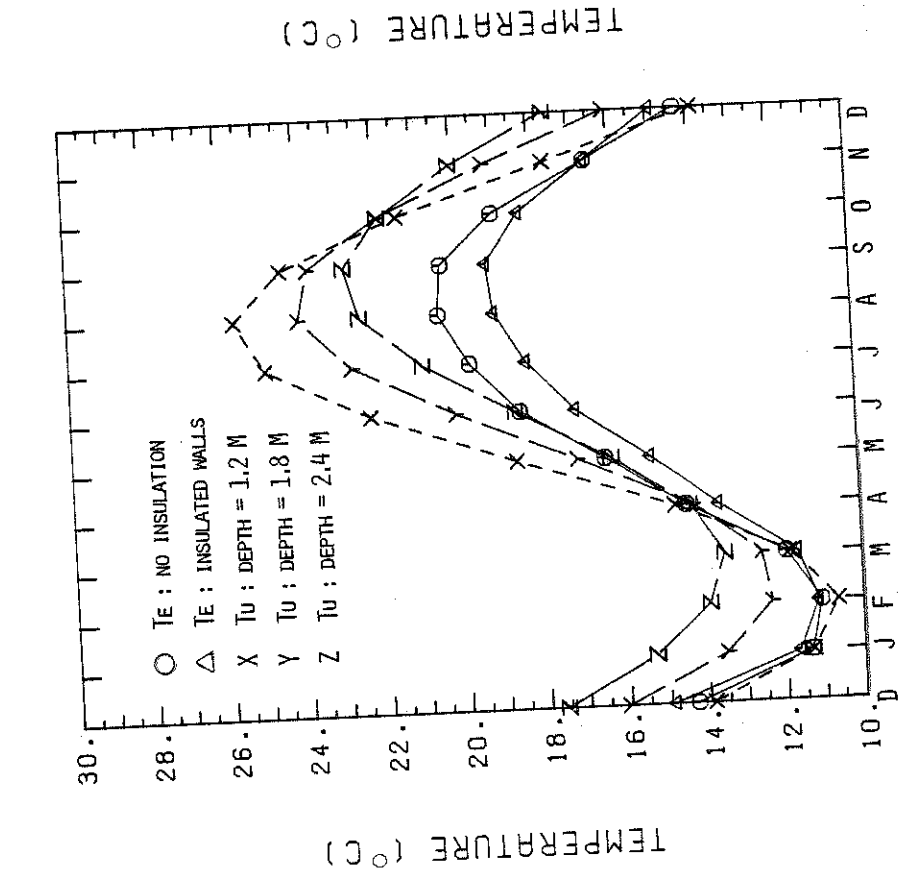


Figure 3.3.3b Wet soil, $k = 8.9 \frac{\text{KJ}}{\text{M hr } ^\circ\text{C}}$

Figure 3.3.3 Undisturbed Earth Temperature, T_u , at Various Depths Compared to the Representative Earth Temperature, T_e , Charleston, S.C.

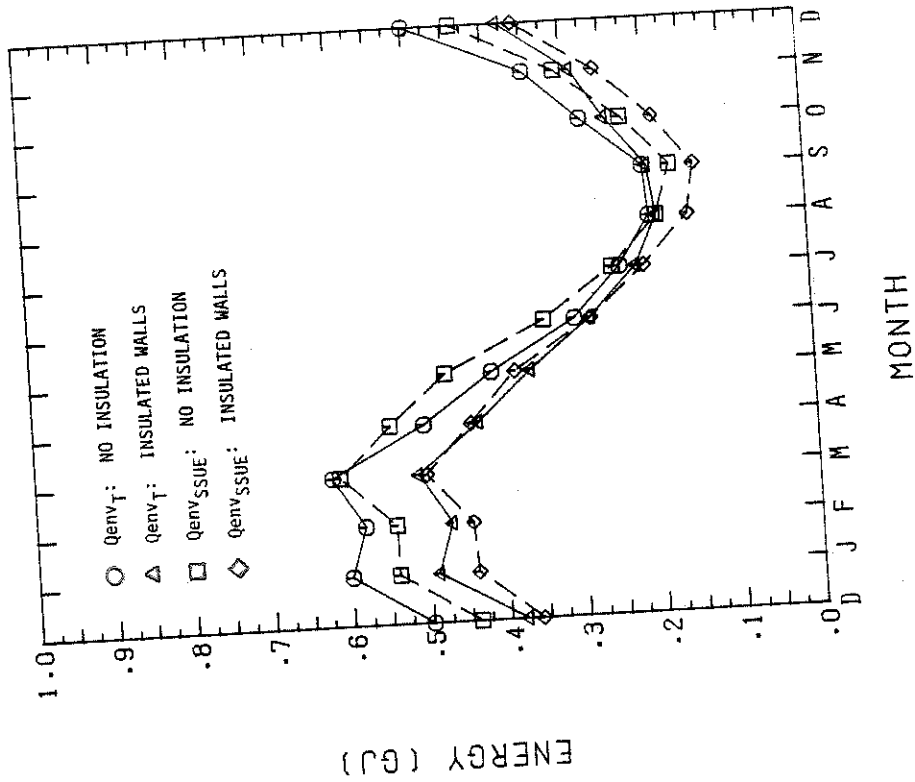


Figure 3.3.4a Transient (T) vs. Steady State Averaging (SSA)

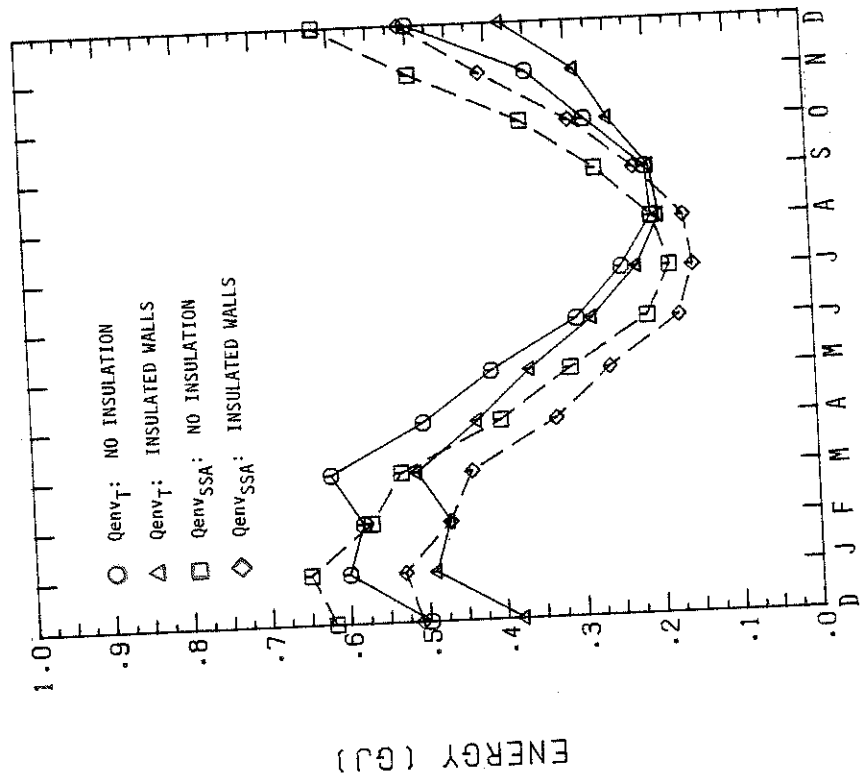


Figure 3.3.4b Transient (T) vs. Steady State Undisturbed Earth (SSUE)

Qenv, Madison, WI.,

Figure 3.3.4 Basement Energy Requirements, Qenv, Madison, WI.,

$$k_{\text{soil}} = 0.9 \frac{\text{KJ}}{\text{M hr } ^\circ\text{C}}$$

Increasing the saturation of the soil adjacent to the basement to one hundred percent causes the deviation of the steady state models to the transient model to increase even further as compared to soils with lower moisture contents. Replacing the transient model by the SSA model yields an error of thirty-five percent and fifteen percent as shown in Figure 3.3.6a. Comparing the SSUE model to the transient model, as illustrated in Figure 3.3.6b, reveals improved agreement with differences of thirty and eleven percent.

From this analysis for Madison, the annual basement heating load is predicted more precisely by the SSUE model for sandy loam soil at saturation levels of twenty-five and one hundred percent. Since most soils exhibit thermal properties between these two soil conditions, the SSUE model is preferred over the SSA model for basement heating load predictions in Madison.

Basement heat transfer comparisons are also analyzed for Charleston. However, a basement in Charleston has both a heating and cooling load to maintain a temperature of 20°C. In the following analysis the annual basement heating and cooling loads predicted by the steady state models, SSA and SSUE, will be compared to the transient model. Deviation of the predicted loads is expressed as a percentage. Comparisons for each steady state model to the transient model at a specified soil condition will have two percentage values stated. The non-insulated basement refers to the first percentage value, whereas the insulated basement, previously defined, refers to the second percentage value. Also, if the devia-

tion is greater than one hundred percent, the comparison is given by the number of times the estimated load is higher or lower than the transient model load calculations.

For dry soil conditions, the SSA model underpredicts the heating load by thirty-six and forty-five percent, compared to the calculations of the transient model, as shown in Figure 3.3.7a. The cooling load requirement calculated by the transient model is small for the non-insulated basement. However, the SSA model overpredicts this load to be eight times the transient model prediction. Also, the insulated basement has no cooling requirement indicated from the transient model, but the SSA model yields a cooling load. The SSUE model underpredicts the heating load by twenty-seven and thirty-six percent, as shown in Figure 3.3.7b, for the same dry soil case. The cooling load, which was only predicted for the insulated basement, is overpredicted by the SSUE model as being thirteen times the cooling load calculated by the transient model. In addition, the SSUE model predicts a cooling load for the insulated basement even though the transient model does not indicate this cooling demand.

If the soil moisture is increased to twenty-five percent saturation, both the basement heating and cooling demands increase. Comparing the heating load predictions of the SSA model to those of the transient model reveals a sixteen percent and eighteen percent overprediction illustrated in Figure 3.3.8a. The cooling load using the SSA model overpredicts by twenty-two percent and a factor of 1.4 as compared to the transient model computations. Heating load estima-

tions by the SSUE model indicate a thirty-two and thirty-four percent difference to the load calculations of the transient model, shown in Figure 3.3.8b. As for the cooling load, calculations indicate an overprediction of twenty-one percent and a factor of 2.8 by the SSUE model compared to the transient model. Thus, for twenty-five percent saturated soil, the SSA model calculates basement loads more accurately than the SSUE model.

If the moisture content of the soil surrounding the basement is increased from twenty-five to one hundred percent saturation, the energy requirements of the basement increase. Annual heating needs are overpredicted by thirty-two and twenty-eight percent using the SSA model to the load values calculated by the transient model as illustrated in Figure 3.3.9a. The significant cooling load predicted by the SSA model differs by eighteen percent and a factor of four as computed by the transient model. For the same soil conditions, the heating load is overpredicted using the SSUE model by fifty-three percent and forty-five percent in comparison to the transient model predictions, as shown in Figure 3.3.9b. The cooling demands are overestimated by the SSUE model being forty-seven percent and a factor of seven higher than the calculations of the transient model. Clearly, the SSA model is more accurate than the SSUE model for this soil condition to estimate both heating and cooling loads of the basement.

Generally, of the two steady state models, more precise energy results for a basement in Madison are predicted by the SSUE model,

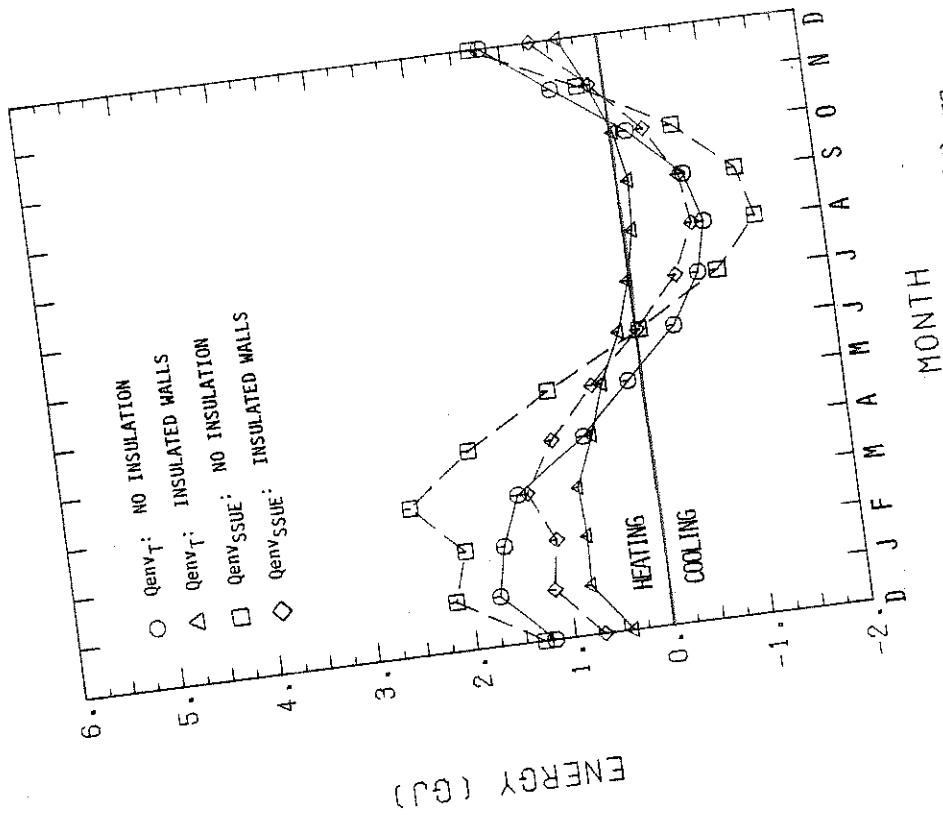


Figure 3.3.9a Transient (T) vs. Steady State Averaging (SSA)

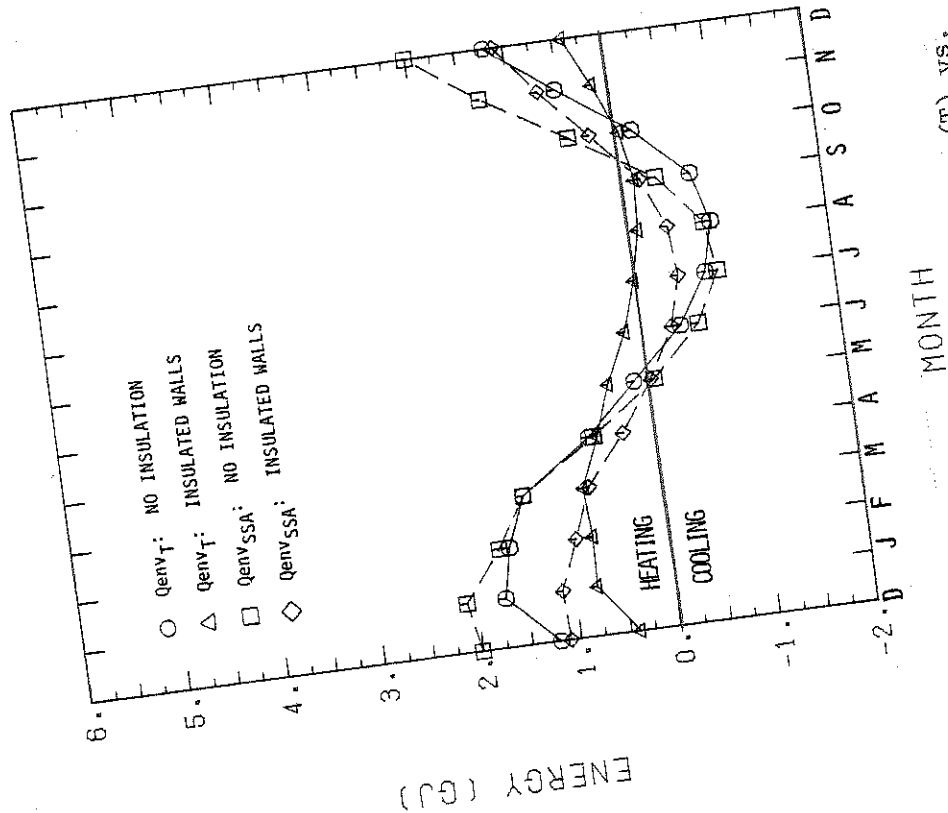


Figure 3.3.9b Transient (T) vs. Steady State Undisturbed Earth (SSUE)

Qenv, Charleston, S.C.,
 $k_{soil} = 8.9 \frac{KJ}{M \cdot hr \cdot ^\circ C}$

two isotherms, as shown in Figure 3.3.1, except the isotherm at the wall is between the insulation and soil. One isotherm exists at the perimeter of the basement between the insulation and the soil at the wall and extends to the floor between the insulation and the soil. The other isotherm exists at the following boundaries: the earth's surface, vertical earth boundary and deep ground. Once the isotherms are defined, calculating S , as discussed in Section 3.2.2, can be readily performed and, therefore, the earth conductance can also be calculated.

In this study the earth conductance, defined in terms of S , is determined by the program EARTH for greater accuracy. A basement-soil system is used as shown in Figure 3.3.1, excluding the insulation where the soil is enclosed by the two isotherms, similar to the graphic technique. This system is allowed to reach equilibrium indicated by the steady state heat flow. For this system the heat flow and the temperature difference between the two isotherms is now known. Using the energy rate expression of Equation 3.2.4, the earth conductance can be calculated. Therefore, the shapefactor conductance can be determined by Equation 3.2.5.

A comparison of the conductances, UA_{sf} , and UA_{ss} , is shown in Figure 3.3.10 for several sandy loam soil conditions as a function of wall insulation thickness. For the basement that is uninsulated, no error exists when replacing UA_{ss} by UA_{sf} . This can be explained by the following observations. The conductance of the non-insulated basement only consists of the soil. Therefore, the isotherm around

the basement perimeter and the isotherm at the exterior earth boundaries, shown in Figure 3.3.1 excluding the insulation, encompass soil only, for both the UA_{ss} and UA_{sf} evaluations. Hence, UA_{ss} is equal to UA_{sf} for an uninsulated basement. Also, as discussed in Section 3.2, UA_{sf} agrees, to a reasonable degree of accuracy, with UA_{ss} for well insulated underground structures. However, for the basement, the insulation is placed on the walls only. The different insulation arrangement in the basement case as compared to the tank case is one reason for the UA_{ss} to UA_{sf} error analysis to yield different results in the two cases.

Assuming the basement heat flow can be approximated by the simple network of Figure 3.3.11, an explanation of the shapefactor conductance UA_{sf} underpredicting the overall conductance UA_{ss} can be provided for the insulated basement. The heat from the basement flows to either of the horizontal boundaries fixed at the same temperature, T_s . The vertical earth boundary used to calculate UA_{sf} normally has a small percentage of the heat flowing across its boundaries and is neglected for this explanation. The energy rate equation for the heat leaving the perimeter of the basement traveling through the soil to the ground surface boundary is expressed as:

$$\dot{Q}_\alpha = UA_\alpha (T_\alpha - T_s)$$

For heat from the basement floor flowing to the deep ground boundary the energy rate equation using Figure 3.3.11 becomes:

3.3.6

3.3.7

$$\dot{Q}_\beta = UA_\beta (T_\beta - T_s)$$

When applied to the earth conductance as computed for the shapefactor conductance, the temperatures T_α and T_β of Figure 3.3.11 must be equal. Unlike the tank case the basement's position in the ground is fixed. Therefore, the conductances UA_α and UA_β , representing the earth conductance, should be fixed assuming the soil conditions are held constant. However, as insulation is added to the walls, a higher percentage of heat will flow through the basement floor. Referring to Figure 3.3.11 and assuming a constant basement heat flow rate, \dot{Q}_β increases while \dot{Q}_α decreases. If the temperatures and conductances are fixed and assuming Equations 3.3.6 and 3.3.7 define the energy rate equations, then \dot{Q}_α and \dot{Q}_β cannot change. Since \dot{Q}_α and \dot{Q}_β actually change, and since T_α and T_β are held constant for the shapefactor conduction, UA_{sf} evaluation, then UA_α and UA_β must change. These earth conductances, UA_α and UA_β , must vary in order to compensate for the shift in heat flow through each circuit.

Since the basement heat flowing to the ground surface travels through less soil, the conductance UA_α is greater than UA_β . For the insulation thicknesses considered, it is assumed that most of the heat flows to the ground surface through \dot{Q}_α rather than the deep ground. Due to the reduction of \dot{Q}_α by adding wall insulation, the decrease in UA_α will cause the earth conductance, part of UA_{sf} , to decrease despite the increase in UA_β . The reduction in the

be investigated. Replacing UA_{ss} by UA_{sf} in Equation 3.3.1 and using T_{av} to estimate T_e will be referred to as the shapefactor averaging (SFA) model. Also, replacing UA_{ss} by UA_{sf} in Equation 3.3.1 with T_u approximating T_e will be referred to as the shapefactor undisturbed earth (SFUE) model.

In Figures 3.3.12a, b and c, the annual basement heating loss calculated by the transient model is compared to the predictions by the SSA, SSUE, SFA and SFUE models. The figures show the predicted heating load requirements for a basement in Madison, Wisconsin, as wall insulation thickness increases for three soil conditions. The comparisons are evaluated for Madison, as opposed to Charleston, because this northern location requires heating all year long. The results are not split into basement heating and cooling which would contribute an additional variable to the comparisons.

All steady state models underpredict the transient model heating load for a basement surrounded by dry soil, shown in Figure 3.3.12a. For this soil case the SSA model is the most accurate steady state model. For twenty-five and one hundred percent saturated sandy loam soil the SFA and SFUE models overpredict and then underpredict the transient model basement heat loss calculations, as shown in Figures 3.3.12b and c. Generally, an overpredicted heat loss is preferred. For this condition the SSUE model predicts the basement heating load most accurately for the partially and totally saturated soil cases. Also, for these two soil conditions, the heating load predicted by the SSA and SSUE models follow the same trans-

ient model heating load trend as the wall insulation thickness increases. For the same two soil conditions, the SFA and SFUE models do not appear as promising since these models begin to underpredict the basement heat loss for wall insulation thicknesses of 0.05 meters and greater. However, for wall insulation thicknesses below 0.076 meters, any of the four models employing Equation 3.3.1 yield basement heat flow in Madison within the following percentage values for the three soil conditions adjacent to the basement:

1. 9%, using dry sandy loam soil
2. 22%, using twenty-five percent saturated soil
3. 35%, using one hundred percent saturated soil.

Specific basement heating predictions for each steady state model compared with the transient model is listed in Table 3.3.2.

3.3.3 Sensitivity Analysis of T_u

Because the basement heat flow predictions by the SSUE model are reasonable, this model is investigated further. From Section 3.3.1 the number of parameters that are a function of T_u was reduced to three; A_a , PO and BO. The specific parameter values used to determine T_u during each month are listed in Table 3.3.3a for Madison and Table 3.3.4a for Charleston. The purpose is to reduce the number of parameters that influence T_u to as few as possible without giving up accuracy. In order to accomplish this, BO and PO are each varied to an upper and lower bound to estimate the influence of these parameters on T_u . The bounds for BO and PO were obtained from a large list of these values calculated for sixty-three United States

locations, by Kusuda and Achenbach [16]. The parameter B_0 is tested at a value of 16.67°C and 8.33°C . The parameter P_0 is varied first to 0.45 radians and then 0.75 radians. The four variations B_0 and P_0 are performed with one parameter changed per case. The temperature profiles from the four cases are compared to the original temperature profile, T_u , used in the analysis of Section 3.3.1. The resulting temperature profiles for Madison are listed in Table 3.3.3b and Table 3.3.4b for Charleston. In these tables the temperatures with the asterisk sign deviate most from the monthly undisturbed earth temperature, T_u , used in the basement heat transfer analysis. The largest error in a temperature difference of 2.4°C when B_0 is 8.33°C in Madison. The second largest temperature difference is 2.14°C when B_0 is 16.67°C in Charleston. Such small temperature variations indicate that generalizing T_u in addition to the simplifications of Section 3.3.1 should yield reasonable monthly temperature predictions. The temperature profiles for each varied parameter case were calculated using Equation 3.3.3. This equation was programmed to obtain results easier and faster. The program is called ETEMP and is listed in Appendix Four.

3.4 Conclusions

Section 3.2 of this chapter discusses simplified techniques to estimate the ground heat loss from a fully mixed, sensible energy, seasonal storage tank. Performance is predicted for a solar space

TABLE 3.3.4a Soil Parameters Used for T_u ; Charleston, S.C.
 Annual Average Air Temperature, $A_a = 18.167$ °C
 Earth Surface Temperature Amplitude, $BO = 12.22$ °C
 Earth Surface Temperature Phase Angle, $PO = 0.49$
 Surface Temperature Diffusivity, $D = 0.0023$ m²/Hr
 Earth Thermal Diffusivity, $x = 1.83$ m
 Depth Below Earth's Surface, $x = 1.83$ m

TABLE 3.3.4b Variation of Soil Parameters; Effect on Temperature, T_u (°C)

Month	Varied Parameter			
	$BO = 16.67$	$BO = 8.33$	$PO = 0.45$	$PO = 0.75$
None				
Jan	11.82	15.00	13.37	14.63
Feb	10.19	14.18	12.28	12.81
Mar	10.51	14.34	12.64	12.23
Apr	12.85	15.51	14.45	13.24
May	16.71	17.44	17.34*	15.63
Jun	20.85	19.51	20.36	18.62*
Jul	24.38	21.27	22.87	21.58
Aug	26.18*	22.17*	24.08	23.59
Sep	25.82	21.98	23.68	24.10
Oct	23.33	20.75	21.76	23.01
Nov	19.55	18.86	18.95	20.66
Dec	15.29	16.73	15.84	17.56

TABLE 3.4.1 Summary of Annual Performance of the Solar Space Heating Systems
Using Seasonal Heat Storage

	Case 1		Case 2		
	(Favorable Tank Parameters)		(Unfavorable transient state)	Tank steady state	shape-factor
Fraction by Solar	0.916	0.922	0.619	0.638	0.595
\bar{Q}_{supp} (GJ)	123.8	124.5	83.7	86.2	80.4
\bar{Q}_{env} (GJ)	11.9	11.8	62.9	61.2	68.3
Average Storage Temperature ($^{\circ}$ C)	51.0	50.9	38.0	37.4	35.6

Both models begin to severely overpredict the monthly fraction of energy supplied to the space heating load by the solar system as the tank parameters become less favorable. Therefore, approximating the seasonal storage tank ground heat loss using either the steady state model or the shapefactor model should be used to evaluate the performance of a solar space heating system using seasonal heat storage on an annual basis.

Section 3.3 of this chapter presents the four simplified models, SSUE, SSA, SFUE and SFA, to evaluate the energy exchange between the ground and a completely below grade basement. Basement heat transfer as predicted by the simplified models is compared to the transient model calculations. The simplified models evaluate basement heat transfer by neglecting the soil thermal capacity and using the steady state rate expression of Equation 3.3.1. The transient model determines the basement ground heat flow by the transient finite difference program, EARTH.

Basement heat flow using the SSA or SSUE model requires the use of a computer or programmable calculator. These two models are compared to the transient model for basement heat flow in two United States locations. The SSUE model yields more accurate results in Madison, Wisconsin, while the SSA model provides more accurate results in Charleston, South Carolina.

Each of the four simplified models is compared with the transient model for the energy requirements of a basement in Madison. The maximum heating load deviation between any of the simplified models

4.0 SUMMARY, CONCLUSIONS AND RECOMMENDATIONS

4.1 The Computer Program, EARTH

A ground coupled heat transfer program, known as EARTH, has been developed. This program computes the energy exchange between the soil and any one of the following earth structures during a specific simulation:

1. A buried seasonal storage tank
2. A completely below grade basement
3. A slab at the ground surface for an above ground building
4. A one story earth sheltered dwelling.

EARTH computes the heat transfer for these structures using a transient, two dimensional, finite difference method in cartesian coordinates. The heat flow crossing any wall of an earth structure or crossing any of the physical boundaries is available to the user. This program is compatible with TRNSYS. However, unlike other TRNSYS subprograms, using EARTH requires a hand drawn diagram of the structure and the surrounding soil.

Calculation of the energy exchange between a structure and the ground using EARTH is based on several assumptions. The primary thermal mechanisms of the soil near the earth structure are simplified to the following heat transfer modes which are used in EARTH:

- c. symmetrical, earth grid required is half of basement or slab and surrounding soil.
3. Earth Sheltered Dwelling
- a. and b. same as "Basement or Slab"
 - c. nonsymmetrical, earth grid required is completed structure and surrounding soil.

For all structures the capacitance effects of the soil are always included.

The predictions using EARTH have been compared to the ground coupling program developed at Georgia Institute of Technology for basement heat transfer analysis [28]. These comparisons reveal the significance of soil capacitance effects.

4.2 Simplified Design Models

The performance of a solar space heating system using an underground seasonal storage tank is simulated in Madison, Wisconsin. Tank heat loss is predicted by two different simplified models; both employ a steady state representation. The models are distinguished by the technique used to compute the combined earth-insulation conductance. The first method, the steady state model, requires a computer or programmable calculator to evaluate the conductance. For the second method, the shapefactor model, the conductance is estimated by a simple hand calculation. System performance using the simplified models is compared to results calculated

the transient model increases as the tank and soil parameters become less favorable. Therefore, performance evaluation of the solar space heating system using either of the simplified models must be analyzed on an annual basis.

Analysis of four steady state models to predict basement heat transfer to the ground have been presented and each of these models is compared to the transient model. Two methods to estimate the monthly representative earth temperature, have been evaluated and yield reasonably accurate temperature values. In the basement analysis the combined earth-insulated conductance is calculated using a computer and by hand. Heat flow predictions determined by the models which use the computer calculated conductance yield results that are closer to the transient model predictions.

Two models, which require a computer to determine the conductance, are compared to the transient model for basement heat flow predictions in Madison, Wisconsin, and Charleston, South Carolina. The first is the steady state averaging (SSA) model which uses a simple method to calculate the monthly earth temperature. The second, the steady state undisturbed earth (SSUE) model requires more information to evaluate the temperature. Generally, the heat transfer predicted by the SSUE model yields more precise results for a basement in Madison, while the SSA model yields better results in Charleston.

Predictions by each of the four simplified models are compared to transient model calculations for annual basement heat loss in

4.3 Recommendations

EARTH allows a significant number of insulation arrangements for a given earth structure-soil system. Because of this capability, insulation design studies can be performed. Computations using EARTH assume the thermal properties of the soil are fixed in time for each zone. However, soil thermal properties change during the year. Because of this, allowing the soil properties to vary with time in EARTH will yield additional heat transfer accuracy (although predicting soil property variations with time is a complex task).

For the tank study, the maximum deviation of the monthly predicted fraction of energy supplied by the solar system is too large using the steady state or shapefactor models. The following revision on the governing energy balance (Equation 3.2.1) will improve monthly predictions. Replace the fixed earth temperature, T_s , by a monthly varying earth temperature as used in the basement analysis.

For the basement study, calculating the earth temperature, T_u , based only on the annual average air temperature, A_a , is the ideal case. However, observing Figures 3.3.12a, b and c, the SSUE model shifts from complete underprediction to complete overprediction of basement heat transfer as soil moisture increases. This implies that the SSUE model and also T_u , is a strong function of the soil thermal diffusivity, D . Therefore, A_a and D should be a function of T_u . Since there is a wide range of soil thermal diffusivities, three values for D are selected. These values

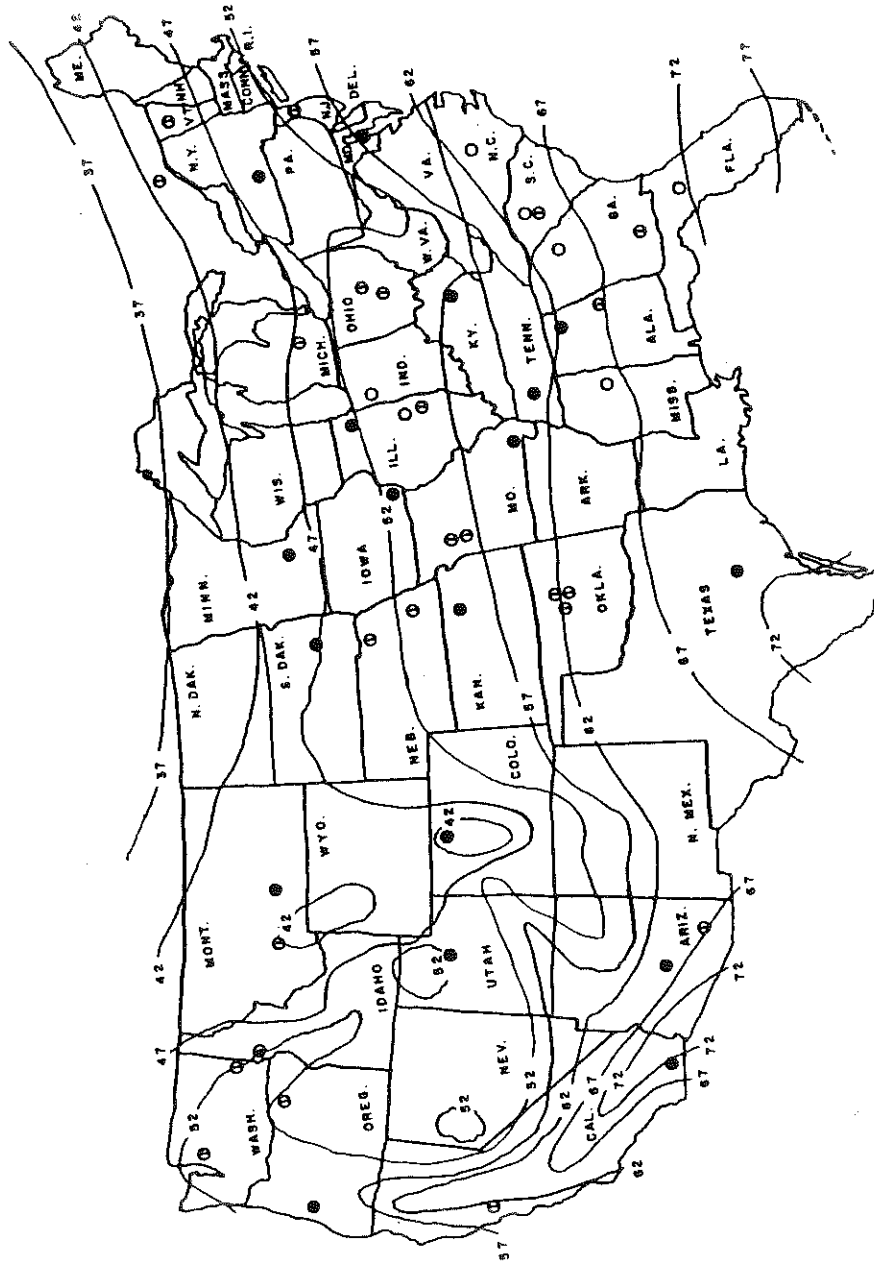


Figure 4.3.1 Well Water, Deep Ground, Isotherms ($^{\circ}$ F) for the 48 Contiguous States [16]

Energy balance at ground surface, T_g , Case 1:

$$(\dot{Q}_{\text{snet}})A + U_1 A (T_{\text{amb}} - T_g) + U_2 A (T_1 - T_g) = 0$$

Separating terms:

$$\dot{Q}_{\text{snet}} + U_1 T_{\text{amb}} + U_2 T_1 - (U_1 + U_2) T_g = 0$$

Solving for T_g :

$$T_g = \frac{\dot{Q}_{\text{snet}} + U_1 T_{\text{amb}} + U_2 T_1}{U_1 + U_2}$$

Substituting for T_g in equation one:

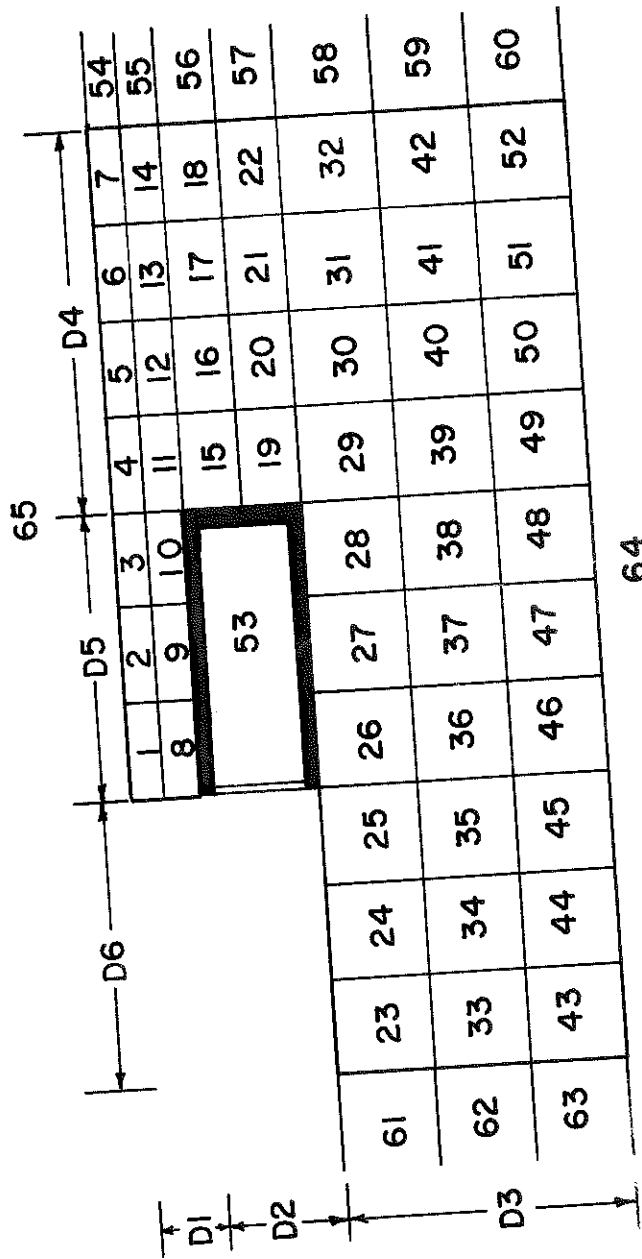
$$T_{\text{sa}} = \frac{U_2}{U_o} \left(\frac{\dot{Q}_{\text{snet}} + U_1 T_{\text{amb}} + U_2 T_1}{U_1 + U_2} - T_1 \right) + T_1$$

After cancelling:

$$T_{\text{sa}} = \frac{\dot{Q}_{\text{snet}}}{U_1} + T_{\text{amb}} + \frac{U_2 T_1}{U_1} - \frac{T_1 (U_1 + U_2)}{U_1} + T_1$$

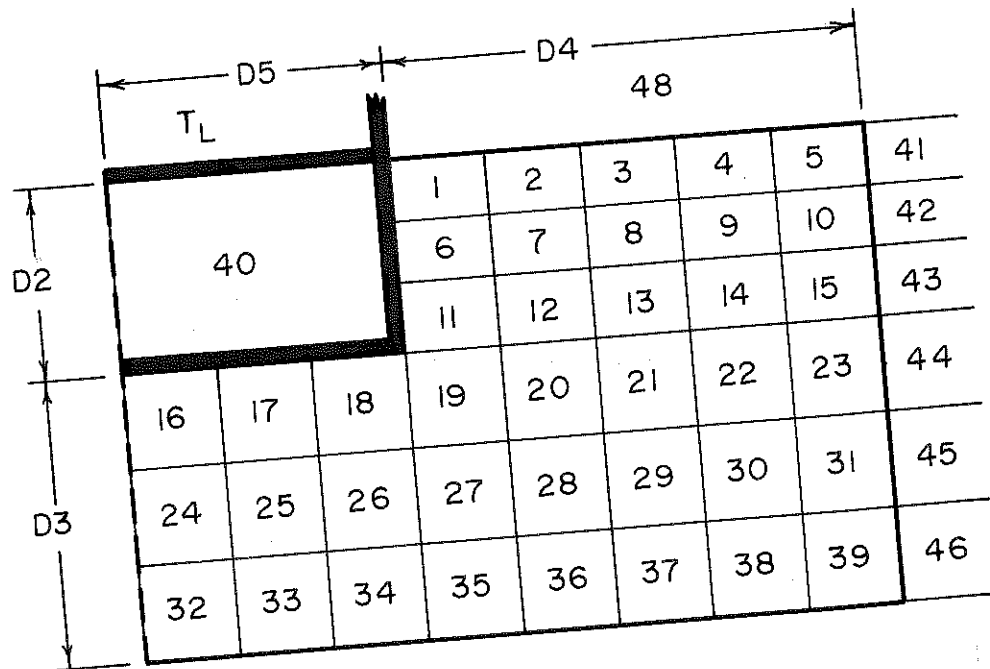
Solving:

$$T_{\text{sa}} = T_{\text{amb}} + \frac{\dot{Q}_{\text{snet}}}{U_1}$$



<u>Boundary</u>		<u>Node Range</u>
Earth Structure		53
Right Boundary		54-60
Left Boundary		61-63
Deep Ground		64
Ambient		65

Figure A.2.1 Node Numbering Sequence - Earth Sheltered Dwelling



47

Boundary

- Earth Structure
- First Floor
- Right Boundary
- Deep Ground
- Ambient

Node Range

- 40
- TL
- 41-47
- 48
- 49

Figure A.2.3 Node Numbering Sequence - Basement

and between a load as shown in Figure A.2.5.

The ground is divided into three zones where the thermal properties of each zone are assumed constant with respect to time and temperature, but may vary from zone to zone, as illustrated in Figures A.2.6 and A.2.7. Various insulation arrangements surrounding the earth structure may be used; Figure A.2.8 displays all possible locations. Any insulation extending into the soil may vary in length as determined by the finite incremental node length in the desired horizontal or vertical direction. The insulation on the vertical wall of the earth structure also has this incremental capability. As for the earth structure floor or ceiling, the entire span is assumed to be covered if insulation is desired.

MATHEMATICAL DESCRIPTION:

The explicit finite difference approximation, (Simple Euler) employed by this model uses the following energy balances.

The buried, sensible energy, fully mixed, seasonal storage tank is represented by the energy balance:

$$\dot{m}_f C_{pf} \frac{T^f - T}{\Delta t} = \dot{Q}_{env} + \dot{Q}_U + \dot{Q}_{SUPP}$$

where:	$\dot{Q}_{env} = \sum_j C_{t,j} (T_j - T_t)$	ground loss rate
	$\dot{Q}_U = \dot{m}_h C_{pf} (T_H - T_t)$	energy rate from heat source
	$\dot{Q}_{supp} = \dot{m}_L C_{pf} (T_L - T_t)$	energy rate to load

The earth sheltered dwelling, basement or slab all assume a fixed earth structure temperature, T_{es} . The energy balance may be thought

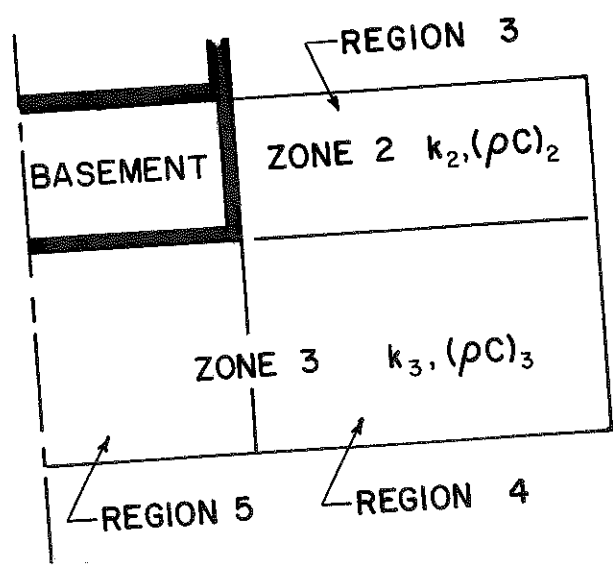
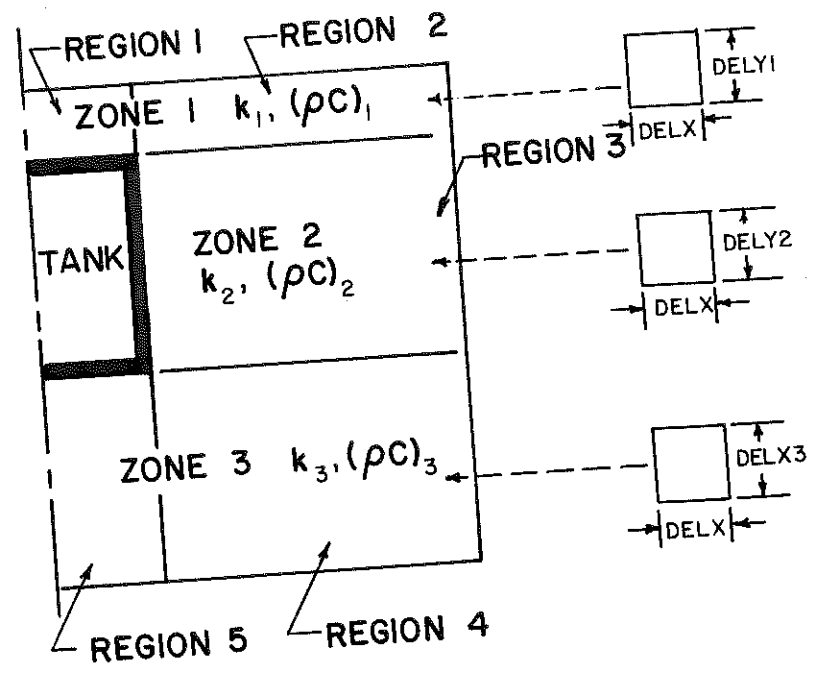


Figure A.2.6 Lumped Thermal Soil Properties - Tank and Basement

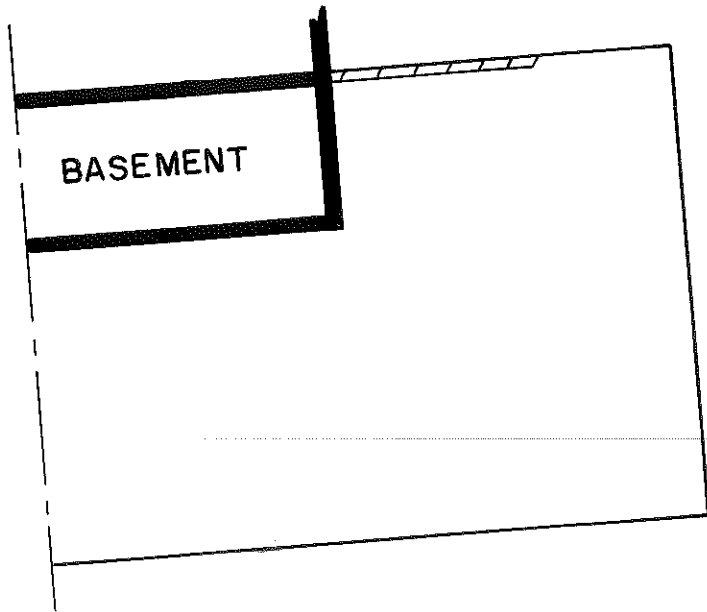
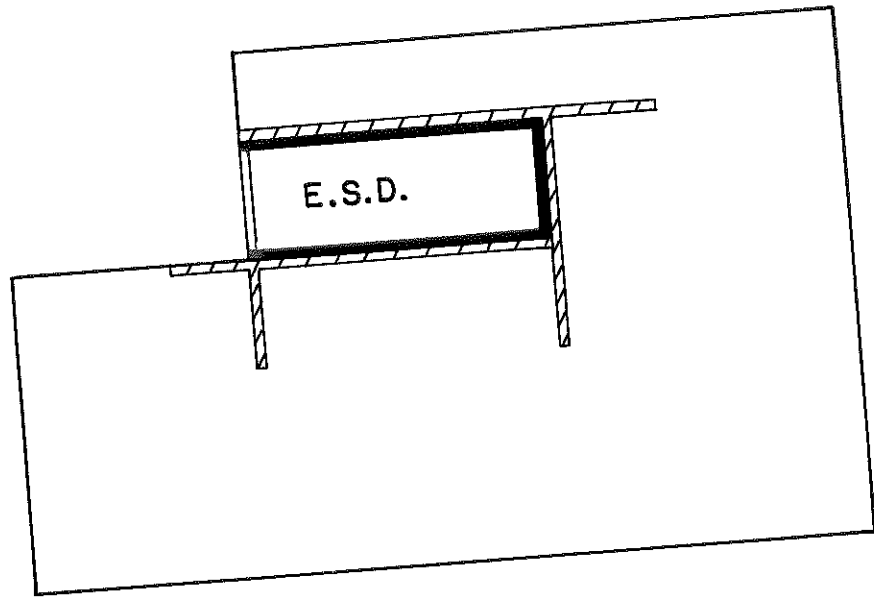


Figure A.2.8 Possible Insulation Arrangements

<u>PARAMETER NUMBER</u>	<u>DESCRIPTION</u>
	or conduction calculations; see Appendix 3)
2	D2 - Vertical height of earth structure; enter zero for slab case
3	D3 - Vertical distance between bottom of earth structure and water table (deep ground sink temperature)
4	D4 - Horizontal distance between right edge of earth structure and right boundary condition nodes.
5	D5 - Horizontal distance of earth structure (only half-width for symmetric cases: Tank, basement or slab)
6	D6 - Distance between left side of earth sheltered dwelling and left boundary condition nodes enter zero for symmetric cases: Tank basement or slab
7	DELY1 - Vertical nodal distance in zone one of grid
8	DELY2 - Vertical nodal distance in zone two of grid
9	DELY3 - Vertical nodal distance in zone three of grid
10	DELX - Horizontal nodal distance of all zones in grid
11	LENGTH - Length of earth structure in "Z" direction 
12	VHC1 - Volumetric heat capacity (ρC_p) of soil in zone one
13	VHC2 - Volumetric heat capacity (ρC_p) of soil in zone two
14	VHC3 - Volumetric heat capacity (ρC_p) of soil in zone three
15	ρ_f - Density of tank fluid
16	C_{pf} - Capacity (specific heat) of tank fluid

<u>PARAMETER NUMBER</u>	<u>DESCRIPTION</u>
	vertical wall may extend in soil, zone 3, between regions four and five) or in soil, zone 3, for slab case
30	YIN3 - Insulation thickness on floor of earth structure adjacent to zone three
31	YIN4 - Insulation thickness (where insulation is spanned horizontally): in soil between zones one and two for tank and earth sheltered dwelling cases; on ground surface for basement and slab cases
32	XIN5 - Insulation thickness (where insulation is spanned vertically): in soil, zone three, between regions five and six. Enter zero for symmetric cases; tank, basement or slab.
33	YIN6 - Insulation thickness (where insulation is spanned horizontally) on soil surface-left side. Enter zero for symmetric cases: tank, basement, or slab
34	DINW - Vertical insulation distance on earth structure wall. Enter zero for slab case
35	DINHR3 - Horizontal insulation distance in soil between zones one and two for tank and earth sheltered dwelling case; on ground surface for basement and slab cases

TRNSYS COMPONENT CONFIGURATION

<u>INPUT NUMBER</u>	<u>DESCRIPTION</u>
1	T_h - Tank case: temperature of fluid from heat source Non-tank case: fixed temperature of earth structure
2	\dot{m}_h - Tank case: mass flow rate from heat source Non-tank case: fix at zero
3	T_L - Tank case: temperature of replacement fluid Basement case: fixed temperature of first floor Earth sheltered dwelling or slab case: fix at zero
4	\dot{m}_L - Tank case: mass flow rate from load Non-tank case: fix at zero
5	T_{amb} - Temperature of environment (ambient)
6	T_{dg} - Deep ground temperature
7	H_{hor} - Total radiation on a horizontal surface
8	T_{dp} - Dew point temperature

TRNSYS COMPONENT CONFIGURATION

<u>OUTPUT NUMBER</u>	<u>DESCRIPTION</u>
1	T_h - Tank case: temperature to heat source Non-tank case: fixed earth structure temperature
2	\dot{m}_h - Tank case: mass flow rate to heat source Non-tank case: zero

<u>OUTPUT NUMBER</u>	<u>DESCRIPTION</u>
16	TEMP; - Instantaneous temperature of desired node number
,	
,	
,	
15+m	TEMP _m - Instantaneous temperature of i th node number

NOTE: For \dot{Q}_{env} , \dot{Q}_t , \dot{Q}_s and \dot{Q}_b positive heat flow is into the earth structure

For \dot{Q}_{rbc} , \dot{Q}_{lbc} , \dot{Q}_{gsink} and \dot{Q}_{asink} positive heat flow is into earth grid

<u>DERIVATIVE NUMBER</u>	<u>DESCRIPTION</u>
-	None

APPENDIX THREE: GRID CHECK

Presented are selected internal values as they appear in the program which are used to detect error as discussed in Chapter Two.

RMCP1 - Inverse of soil thermal capacity in zone one $\left(\frac{1}{\rho C_p V}\right)_1$

RMCP2 - Inverse of soil thermal capacity in zone two $\left(\frac{1}{\rho C_p V}\right)_2$

RMCP3 - Inverse of soil thermal capacity in zone three $\left(\frac{1}{\rho C_p V}\right)_3$

RMCPF - Inverse of fluid thermal capacity for tank $\left(\frac{1}{\rho C_p V}\right)_f$

NH1 - Number of rows in zone one

NH2 - Number of rows in zone two

NH3 - Number of rows in zone three

NV1 - Number of columns in region two or three or four

NV2 - Number of columns in region one or five

NV3 - Number of columns in region six

DELY1 - Vertical node distance in zone one

DELY2 - Vertical node distance in zone two

DELY3 - Vertical node distance in zone three

NVTZ1 - NV1 + NV2

NVT - NV1 + NV2 + NV3

NHT - NH1 + NH2 + NH3

NNTE - Number of nodes in earth grid (excluding all boundary condition nodes)

NBCL3 - Last right boundary condition node number adjacent to zone three

NESBCF - First earth shelter (left) boundary condition node number adjacent to zone three

NESBCL - Last earth shelter (left) boundary condition node number adjacent to zone three

NNINW - Number of nodes that have vertical wall insulation

NNHR3 - Number of nodes horizontally insulated at top of region three

NNHR4 - Number of nodes horizontally insulated at top of region four (slab case only)

NNVR4 - Number of nodes vertically insulated between regions four and five of zone three

NNVR5 - Number of nodes vertically insulated between regions five and six of zone three (earth sheltered dwelling only)

NNHR6 - Number of nodes horizontally insulated at top of region six (earth sheltered dwelling only)

COND1 - Thermal conductivity values of the 19 combinations as
'
' defined in the program listing or as shown in Figures
'
' 2.4.2 and 2.4.3
COND19

NOTE: An earth grid sketch is found in appendix two
for all four earth structures

```

SUBROUTINE TYPE7(TIME,XIN,OUT,I,DTDT,PAR,INFO)
REAL MDOYH,MDOYL
DIMENSION XIN(25),OUT(300),TNEW(300),PAR(300),INFO(10)
DIMENSION TT(300,50),C(300,50),Q(300),TOLD(300),TS(300)
DIMENSION TSTART(300),DE(300)
COMMON/SIM/TIME0,TFINAL,DELT
C.....PROGRAM EARTH
C.      THIS IS A TWO DIMENSIONAL TRANSIENT GROUND COUPLING PROGRAM
C.      USING FINITE DIFFERENCE APPROXIMATION; CONDUCTION THROUGH
C.      THE EARTH, CONVECTION AT THE WALL INTERFACE AND GROUND SURFACE,
C.      AND RADIATION AT THE GROUND SURFACE. THIS PROGRAM CAN MODEL
C.      FOUR CONFIGURATIONS OF EARTH STRUCTURES WHICH ARE:
C.          1. ONE STORY EARTH SHELTERED DWELLING (E.S.D.)
C.          2. SEASONAL STORAGE TANK
C.          3. COMPLETELY BELOW GRADE BASEMENT
C.          4. SLAB, OF AN ABOVE GRADE BUILDING.
C.      ONE NODE EARTH STRUCTURE; VARIABLE EARTH NODE SIZE
C.      D1,2,3;VERTICAL HEIGHT ABOVE,ADJACENT,BELOW EARTH STRUCTURE
C.      BASEMENT STUDY; INPUT D1=0. SLAB STUDY; INPUT D1=0. AND D2=0.
C.      D4;DISTANCE FROM STRUCTURE TO RIGHT B.C. NODES
C.      D5;WIDTH OF EARTH STRUCTURE
C.      D6;DISTANCE FROM E.S.D. TO LEFT B.C. NODES
C.      LENGTH;THIRD SPACE VARIABLE DISTANCE
C.      IF(INFO(7),GE,0)GO TO 500
C.      *** FIRST CALL OF SIMULATION ***
C.      PARAMETERS
C.      D1=ABS(PAR(1))
C.      D2=PAR(2)
C.      D3=PAR(3)
C.      D4=PAR(4)
C.      D5=PAR(5)
C.      D6=PAR(6)
C.      DELY1=PAR(7)
C.      DELY2=PAR(8)
C.      DELY3=PAR(9)
C.      DELX=PAR(10)
C.      LENGTH=PAR(11)
C.      NODE NUMBERING
C.      R2 NODE SIZE=R1 NODE SIZE
C.      DELX SAME IN R1-6
C.      NV1:NO. OF VERT. COLUMNS IN REGION 2,3 & 4
C.      NV2:NO. OF VERT. COLUMNS IN REGION 1 & 5
C.      NV3:NO. OF VERT. COLUMNS IN REGION 6
C.      NH1:NO. OF HORIZ. ROWS IN REGION 1 & 2
C.      NH2:NO. OF HORIZ. ROWS IN REGION 3
C.      NH3:NO. OF HORIZ. ROWS IN REGIONS 4 & 5
C.      DELY1,2,3;NODE HEIGHT ZONE 1,2,3
C.      NH1=IFIX(D1/DELY1+0.001)
C.      IF(D1,EQ,0.0)NH1=0

```

```

      IF(D6, EQ, 0.0) NBLC6=0
C.   NBCF1: RIGHT BOUNDARY CONDITION FIRST NODE ZONE 1
C.   NBCL1: RT, B.C. LAST NODE Z1
C.   NBCF2: RT, B.C. FIRST NODE Z2
C.   NBCL2: RT, B.C. LAST NODE Z2
C.   NBCF3: RT, B.C. FIRST NODE Z3
C.   NBCL3: RT, B.C. LAST NODE Z3
C.   NESBCF, NESBCL: E.S.D. B.C. FIRST NODE, LAST NODE (LEFT SIDE)
      NBCF1=NNTET+1
      NBCL1=NNTET+NH1
      IF(D1, EQ, 0.0) NBCF1=0
      IF(D1, EQ, 0.0) NBCL1=0
      NBCF2=NNTET+NH1+1
      NBCL2=NNTET+NH1+NH2
      IF(D2, EQ, 0.0) NBCF2=0
      IF(D2, EQ, 0.0) NBCL2=0
      NBCF3=NNTET+NH1+NH2+1
      NBCL3=NNTET+NH1+NH2+NH3
      NESBCF=NNTET+NHT+1
      NESBCL=NNTET+NHT+NH3
      IF(D6, EQ, 0.0) NESBCF=0
      IF(D6, EQ, 0.0) NESBCL=0
C.   LTI: NUMBER OF TEMP. VALUES TO BE ENTERED
C.   LTNO: NO. OF NODES FOR WHICH TEMP. HISTORY IS PRINTED
      LTI=PAR(39)
      LTNO=PAR(39+LTI+1)
      NI=8
      NP=39+LTI+LTNO+1
      NO=0
      CALL TYPECK(1, INFO, NI, NP, NO)
C.   PARAMETERS (CONTINUED)
C.   VHC1,2,3: VOLUMETRIC HEAT CAPACITY OF SOIL, ZONES 1,2 AND 3
C.   (DENSITY*SPECIFIC HEAT)
C.   RHOF: DENSITY OF FLUID
C.   CAPF: CAPACITY OF FLUID
C.   TVOL: TANK VOLUME
C.   TK1,2,3, IN, C: THERMAL CONDUCTIVITY ZONE 1,2,3, INSULATION, WALL
C.   HAMR: HT. TR. COEFF. AMBIENT
C.   HROOM: HT TR. COEFF. BASEMENT
C.   YC1,3, XC2: WALL THICKNESS ADJACENT TO ZONE 1,3,2
C.   YIN1,3, XIN2: INSULATION THICKNESS ADJACENT TO ZONE 1,3,2
C.   XIN2 MAY APPLY FOR DEPTHS BEYOND VERTICAL WALL
C.   YIN4: INSULATION THICKNESS BETWEEN R2 AND R3
C.   XIN5: INSUL. THICKNESS BETWEEN R5 AND R6 (E.S.D. CASE)
C.   YIN6: INSUL. THICKNESS BETWEEN R5 AND AMBIENT
C.   DINW, DINVR4: VERT. INSUL. DISTANCE 1 ON WALL OF BASEMENT; INTO R4
C.   DINHR3: HORIZ. INSULATION DISTANCE IN R3; OR R4 FOR SLAB CASE
C.   DINVR5: VERT. INSUL. DISTANCE LEFT SIDE OF R5 (E.S.D. CASE)
C.   DINHR6: HORIZ. INSUL. DISTANCE OF R6 (E.S.D. CASE)
      VHC1=PAR(12)

```